ISTANBUL TECHNICAL UNIVERSITY ★ GRADUATE SCHOOL OF SCIENCE ENGINEERING AND TECHNOLOGY

HEAVY DUTY DIESEL ENGINE
THERMO MECHANICAL FATIGUE ANALYSIS

M.Sc. THESIS

Şener KANTÜRER

Department of Mechanical Engineering

Solid Mechanics Programme

JUNE 2012

ISTANBUL TECHNICAL UNIVERSITY ★ GRADUATE SCHOOL OF SCIENCE ENGINEERING AND TECHNOLOGY

HEAVY DUTY DIESEL ENGINE THERMO MECHANICAL FATIGUE ANALYSIS

M.Sc. THESIS

Şener KANTÜRER
(503081513)

Department of Mechanical Engineering

Solid Mechanics Programme

Thesis Advisor: Prof. Dr. Ata MUGAN

JUNE 2012

İSTANBUL TEKNİK ÜNİVERSİTESİ ★ FEN BİLİMLERİ ENSTİTÜSÜ

AĞIR VASITA DİZEL MOTORUNUN TERMOMEKANİK YORULMA ÖMRÜ ANALİZİ

YÜKSEK LİSANS TEZİ

Şener KANTÜRER
(503081513)

Makina Mühendisliği Anabilim Dalı

Katı Cisimlerin Mekaniniği Programı

Tez Danışmanı: Prof. Dr. Ata MUĞAN

HAZİRAN 2012

Şener KANTÜRER, a M.Sc. student of ITU GRADUATE SCHOOL OF SCIENCE ENGINEERING AND TECHNOLOGY, student ID 503081513, successfully defended the thesis entitled "HEAVY DUTY DIESEL ENGINE THERMO MECHANICAL FATIGUE ANALYSIS" which he prepared after fulfilling the requirements specified in the associated legislations, before the jury whose signatures are below.

Thesis Advisor :	**Prof. Dr. Ata MUGAN** İstanbul Technical University	....
Jury Members :	**Prof. Dr. Ata MUGAN** İstanbul Technical University	....
	Prof. Dr. Ekrem TUFEKCI İstanbul Technical University	....
	Assistant Prof. Dr. Nuri SOLAK İstanbul Technical University	....

Date of Submission : 04 May 2012
Date of Defense : 15 June 2012

FOREWORD

I would like to express my deep appreciation and thank my advisor Prof. Dr. Ata MUGAN who made this thesis possible. This work could not have been completed without his support and invaluable advice.

I would like to thank colleagues in Ford Otosan for their technical support and advices during the modeling of this study.

Also, I would like to thank my friend Şeyda HATİBOĞLU for her patience and support during my study.

Last but not least, I would like to thank my family for their encouragement and assistance over my life.

June 2012

Şener KANTÜRER
(Mechanical Engineer)

TABLE OF CONTENTS

ABBREVIATIONS

CAD	**:**	Computer-Aided Drawing
CAE	**:**	Computer-Aided Engineering
CFD	**:**	Computed-Flued Dynamics
TMF	**:**	Thermo-Mechanical Fatigue
NVH	**:**	Noise, Vibration and Harshness
HP	**:**	High Pressure
DoE	**:**	Design of Experiment
LCF	**:**	Low Cycle Fatigue
PFP	**:**	Peak Fire Pressure
ECU	**:**	Electronical Control Unit
EGR	**:**	Exhaust Gas Recirculation
LH	**:**	Left Hand
RH	**:**	Right Hand
CW	**:**	Clock Wise
FEA	**:**	Finite Element Analysis
DOF	**:**	Degree of Freedom
SAE	**:**	Society of Automotive Engineers International

LIST OF TABLES

Page

LIST OF FIGURES

LIST OF SYMBOLS

k	: Initial yield stress
K	: Bulk Modulus
n	: Material parameter
D	: Damage parameter
P’	: The rate of the equivalent strain
S'	: Deviatoric part of stress (differential stress)
X'	: Deviatoric part of back stress (differential stress)
J(a)	: Invariant
R	: Isotropic hardening
X	: Kinematic hardening
S	: Material parameter
E	: Young modulus
V	: Poison ratio

NOTATION

Tensor notation is used where boldface symbols indicate tensors. Their order becomes clear out of the context. The summation convention is adopted and the following operations are used:

$a : b = a_{ij}\, b_{ij}$

$(a \otimes b)_{ijkl} = a_{ijkl}\, b_{ijkl}$

$(c : b)_{ij} = c_{ijkl}\, b_{kl}$

$(c : d)_{ijkl} = c_{ijmn}\, d_{mnkl}$

The unity tensors are

1	second order unity tensor
I	fourth order unitiy tensor

Additionally the following operators are used:

a_m	mean of a second order tensor a_{ij} ($a_m = 1/\,3a_{kk}$)
a'	deviator of a second order tensor a_{ij} ($a' = a - a_m 1$)
c^{-1}	inverse of a tensor c ($c : c^{-1} = c^{-1} : c = I$)
y’	material time derivative of a scalar or tensorial variable y
$[y]_{max}$	current maximum value of a scalar variable

HEAVY DUTY DIESEL ENGINE THERMO MECHANICAL FATIGUE ANALYSIS

SUMMARY

In recent years, automotive industry faces a difficult and versatile problem such as producing more economical engines with higher performance according to customer expectations while reducing exhaust emissions due to legal regulations and environmental concerns. The main objective is to manufacture silent, cheaper and lighter new generation green engines with low exhaust emissions which also show higher performance and consume less fuel. All these expectations have solved partially by increasing the peak firing pressure and modifying the design. However, thermal fatigue occurring during the start-stop cycle has become an important issue that should be taken into consideration more carefully with these modifications, increasing internal pressure and working temperature inside engines. Currently used gray cast iron as cylinder head and block material is insufficient to provide general expectations so new materials should be used or developed. Material problems began to unravel with the use of vermicular cast iron (CGI, GJV450) and aluminum alloys (ex. Al319-T7B) for engine blocks and cylinder heads. The density of aluminum alloys is much lower than grey cast iron and using a smaller amount of vermicular cast iron provides same or even better performance in low thickness with its better mechanical properties.

In addition to material upgrade of the material, it is important to prove out their performance and life spending less time and cost. The 60%-70% cost of "Development of engine and transmission components" is due to the validation tests. Projects which created with the help of traditional product development mentality, analytical calculations and previous experiences requires a large number of tests, are the reason for the high cost. The percentage of computer-aided analysis in the product development budget is seriously low (expressed in terms of a few percent) because of carrying on old methods in some areas and lack of usage. It is possible to achieve great profit in the design with correct approaches and applications if the progress in the methods and their fewer prices when compared to tests is considered. In recent years, design studies on this subject are carried out significantly. Computer-aided analysis of gray cast iron parts indicated successful results, however results for the vermicular cast iron which is newly used in automotive industry are not reliable at the same rate. The main reason for this difference is the assumption of material constants same for all parts for the classical approach, whereas vermicular cast iron has heterogeneous microstructure (nodularity) which formed due to varying cooling rate with the cross section. Companies develop their own experimental data for the identification of cross-sectional properties and sharing information is almost never made. Thermal and mechanical loadings become more obvious due to non-homogenous microstructure of cylinder head which consist of a combination of thin and thick sections of complex geometrical parts.

Engine blocks and/or cylinder heads are subjected to verification/performance tests in the dynamometer after the design stage. Despite being expensive, dynamometer tests are the basic test approach for all engine manufacturers. The necessity of collecting the prototype engine and long test periods with standard fuels like thousands of hours are the reason for expensive tests. In general, a test lasts for months and thousands of liters of fuel consumed during that time. Design results can be obtained too slowly because of this long period of experiments, sometimes effect of a small change can be observed for months.

In this study, the aim is the simulating thermal-mechanical fatigues which is going to be used for modeling of cylinder head, one of the most complex parts of new generation engines. In this way, any type of cylinder head produced from different materials may be analysed faster and more economically without the need to collect engine. In addition to cost advantages, pollution created by combustion of thousands liters of fuels will be reduced by using gaseous fuels such as natural gas because diesel/gasoline is not used as fuel, thus an environmentally friendly test method will be developed for green engines.

AĞIR VASITA DİZEL MOTURUNUN TERMOMEKANİK YORULMA ÖMRÜ ANALİZİ

ÖZET

Otomotiv endüstrisi son yıllarda, yasal düzenlemeler ve çevresel kaygıların etkisiyle egzoz emisyonlarını azaltırken; müşteri beklentileri doğrultusunda da daha yüksek performansta ekonomik motor üretmek gibi zor ve çok boyutlu bir problemle karşı karşıyadır. Temel hedef, daha az yakıt tüketen, yüksek performanslı ve düşük egzoz emisyon değerlerine sahip yeni nesil çevreci motor üretimidir. Düşük maliyet, hafiflik ve sessiz çalışma ise diğer ön plana çıkan beklentilerdir. İç basıncın arttırılması ve dizayn değişiklikleri ile tüm bu beklentilerin büyük çoğunluğuna çözüm bulunmuştur. Ancak dizayn değişiklikleri, artan iç basınç ve çalışma sıcaklığı motorlarda start-stop çevrimi esnasında meydana gelen düşük çevrimli termomekanik yorulmayı çok daha fazla dikkat edilmesi gereken bir sorun haline getirmiştir. Halihazırda silindir kafası ve bloğu için kullanılan gri dökme demir genel beklentileri sağlamakta yetersiz kalmakta yeni malzemelerin kullanımı/geliştirilmesi gerekmektedir. Malzeme problemi, vermiküler dökme demir (CGI, ör. GJV450) ve alüminyum alaşımlarının (ör. Al319-T7B) motor blokları ve silindir kafalarında kullanılmasıyla çözülmeye başlamıştır. Alüminyum alaşımları gri dökme demire oranla çok daha düşük bir yoğunluğa sahipken vermiküler dökme demir daha iyi mekanik özellikleri sayesinde daha az miktarda (ince kesitte) kullanılarak aynı hatta daha iyi performans sağlamaktadır.

Gerçekleştirilen bu çalışmada silindir kafasının ömür hesabının yapılması için mekanik ve termal etkiler gerçekçi bir şekilde modellenmiştir. Bilgisayar destekli mühendislik teknolojileri kullanılarak başta silindir kafası ve motor bloğu parçalarının mekanik ve termal yükler altındaki davranışı göz önüne alınarak numerik modeller ve geliştirmeler kullanılmıştır. Bu bilgisayar destekli mühendislij metodolojisi, 1-boyutlu ve 3-boyutlu analitik araçlar kullanılarak motor içi akışkanın modellenmesini ve motor parçalarının yapısal olarak modollenmesini içeriyor.

Motor geliştirme projeleri genelde sıfırdan bir geliştirme projesinden ziyade, projelerin devamında yapılan dizayn ve doğrulama prosesi önce yapılmış hesaplara ve varsayımlara dayanır. Hesaplamalar, gerçekleşecek değişiklikleri içerirler. Bu yüzdendir ki, dizayn gereksinimleri uygulamadan uygulamaya ve kalibrasyon tipine göre değişkenlik gösterebilir.

Yapılan en küçük bir değişiklik dahi, silindir kafasındaki sıcaklık ve gerinim dağılımını önemli ölçüde değiştirerek, motor ömrünü kabul sınırlarının altında kalmasına neden olabilir. Bu nedenle motor üzerinde gerçekleştirilen çalışmalarda silindir kafası en önemli madde olarak sürekli kontrol altında tutulmaktadır.

Motorun her ısınıp soğuması bir ısıl çevrime karşılık gelir. Bir motorun bu yükler altında dayanımı motordan motora, sürücüden sürücüye değişkenlik arzeder. Yine de her motor belli sayıdaki ısıl çevrime direnç gösterecek şekilde tasarlanır. Silindir

kafasının ısıl yorulması mekanik gerinim, sürünme ve oksidasyon gibi bir çok farklı mekanizmanın aynı anda çalışması ile gerçekleşen kompleks bir fenomendir

Termomekanik yorulma hesabının gerçekleştirilmesi için bir çok disiplinin birlikte çalışması gerekmektedir. Tezin yazımında kurulan kurguda bu disiplinlere sırayla yer verilmektedir. Tezin metodolojisinde, basamak basamak hangi komponent ve sistemlerin ne şekilde modelleneceği anlatıldı. Kurulan analiz modelleri, kullanılan malzeme ve bu malzemenin matematiksel modellenmesine sırayla yer verildi.

Silindir kafa malzemesi olarak kullanılan CGI malzemenin davranışının incelenmesi için Chaboche teorisi kullanılmıştır. Chaboche teorisi gerilme/gerinim bazlı olup, artımlı plastisite teorisine dayanan son derece kapsamlı bir modeldir. Analizlerimiz esnasında chaboche malzeme teorisini kullanan bir alt program kullanılmıştır. Bu alt program silindir kafası için ömür hesabını gerçekleştirmektedir.

Diğer bir önemli nokta da malzeme testleridir. Thomat alt programı kullanılacak malzeme için yapılmış bir ön değer seti ile kullanılmaktadır. Buna karşın, belli bir silindir kafası için elde edilmiş ve başarılı sonuçlar vermiş TMF parametreleri, aynı malzemeden yapılmış farklı bir mimariye sahip başka bir silindir kafası için aynı derecede başarılı sonuçlar vermeyebilir. Dökümhane farklılığı da bu varyasyona olumsuz yönde etki edecek önemli bir unsurdur. Bir kez imalatçı seçilip prototip kafalar üretildikten sonra, bu kafalardan çekilecek numunelerle ek testler yapılacak ve tüm parametreler korale edilmesi gerekmektedir. Bu hem döküm kalitesini değerlendirme hem de başarılı ömür tahmini yapabilme imkanı veremektedir.

Bir diğer konu ise sıcaklığın modelimize eklenmesidir. Sıcaklık, malzeme karakterizasyonuna ve motorun ömrüne etki eden en önemli parametredir. Bu yüzden motorun çalışma koşullarındaki sıcaklık dağılımının en doğru şekilde hesaplanması ve bu hesapların test sonuçları ile korele edilmesi analizlerin doğruluğu bakımından önemlidir. Sıcaklıkların doğru hesaplanabilmesi için motor sıcaklığına doğrudan etki eden soğutma suyunun etkisinin doğru şekilde modellenmesi gerekmektedir.

Bu çalışmada konjuge kafa/blok analizleri gerçekleştirilmiştir. Bu tip ayrık analiz metodu özellikle konsept fazı gibi akışkan yüzeylerinde çok fazla iterasyon gerektiren tasarım çalışmaları için özellikle uygundur. Bu nedenle konsept motor geliştiren şirketlerin tercihi olmuştur.

Motor bloğu ve silindir kafasını modellerken, gerçekleştirilmesi gereken diğer bir iş de soğutma ceketlerinin hesaplamalı akışkanlar dinamiği (Computational Fluid Dynamics - CFD) metodları ile modellenmesidir. Dizel motorlarında silindir içindeki ortalama gaz sıcaklıkları 1000 C° dereceyi aşan sıcaklıklara ulaşmakta ve bu değer daha verimli motor arayışıyla her geçen gün artmaktadır. CFD metodları soğutma sıvısı ve metal yüzeyler arasındaki konveksiyon katsayısı dağılımını ve kanal içerisinde soğutma sıvısı sıcaklık dağılımını hesaplamakta kullanılır. Bu veriler termal analizde sınır değerleri olarak kullanılır ve blok ve silindir kafasındaki sıcaklık dağılımını belirler.

Silindir kafası ve motor bloğu analizlerinde diğer bir önemli ilerleme silindir için yanma modellerinin sonuçlarının doğrudan yanma yüzeylerine beslenmesidir. Mevcut metod 1D termodinamik analiz sonuçlarının kafa ve blok yüzeylerine elle girilmesi ile gerçekleştirilir. Kafa enjektör çevresinde bir kaç bölgeye bölünür ve buraya termodinamik analiz sonucu ısıl katsayılar ve gaz sıcaklıkları uygulanır. Bu nedenden dolayı enjektör sprey açısı ve konumu gibi etkileri görmek mümkün değildir. Örnek olarak bir spreyin altında kalan bölgenin normalden daha sıcak olması beklenirken mevcut analzi metodunda bunlar görülmemektedir. Modellenen yanmanın doğrudan silindir alt yüzeyine tanımlanması (mapping) buna imkan verecektir.

Sonlu elemanlar yöntemi ile beraber altmodelleme (submodel) yöntemi de çalışmalarımız esnasında geliştirildi. Kurulan modellerin milyonun katları kadar eleman içermesinden dolayı analiz sürelerini çok uzun olması beklenmektedir. (100-120 saat civarında) Çalışmak istediğimiz bölgeleri motor üzerinde belirleyerek kuracağımız altmodeller çok daha kısa sürede istediğimiz sonuçları almamızı sağlamıştır. Bu modelleme yeteneği ile beraber daha verimli çalışma süreleri elde edilerek, kullanılan yazılımların lisans masrafları önemli derece de azaltılmıştır.

Bu tez çalışmasının sonucunda, geliştirilen veya tasarlanan bir konsept motor için kritik olan silindir kafasının termomekanik olarak yorulma ömrü hesaplandı. Bu şekilde çok maliyetli olan prototip ürün ve motor testlerine gerek kalmadan bu tez metodolojisiyle yorulma ömrünün tespit edilmesi gerçekleştirilmiştir.

1. INTRODUCTION

This study attempts to capture the current practice for thermo mechanical fatigue analysis (TMF) of the cylinder head assembly and the top of the cylinder block. This study are based upon a general TMF. The model is built to identify of any special problem by detailing of the assumpions. Detailing of the assumotions may requires any deviation which should be consulted with the relevant technical specialists.

The solver used for both the thermal and structural analysis is ABAQUS. The basic TMF process involves a thermal analysis, with linear elements, followed by a linear-elastic analysis of the structural model, with parabolic elements.

The first step is to create a Finite Element (FE) model of the engine assembly to be used in the thermo-mechanical analysis. A single FE model should be created which contains the cylinder head and block assembly using parabolic tetrahedral elements and include both thermal and structural boundary conditions. From this FE model, unnecessary elements, nodes and boundary conditions should be deleted when either a thermal or structural deck are required to be written out. The use of one model to contain all the information for both the thermal and structural analyses means that if design changes are required, then it is only necessary to modify one model.

Several techniques are available to assist in the management of large models. Sub-modeling technique is a well known technique in finete element method for managing large models. This technique is applied to the analysed model in this study. Sub-modeling allows the analyst to focus on a subset of a model based on an existing solution from a global model.

In the present study, mechanism-based models are developed to describe the time and temperature dependent cyclic plasticity and damage of cast iron materials. The cyclic plasticity model is a combination of a viscoplastic model with kinematic hardening and a porous plasticity model to take the effect of graphite inclusions into account. Thus, the model can describe creep, relaxation and the Bauschinger-effect as well as the tension-compression asymmetry often observed for cast iron. The model for thermomechanical fatigue life prediction is based on a crack growth law, which assumes that the crack growth per cycle, da=dN, is correlated with the cyclic crack tip opening displacement, ΔCTOD. The effect of the graphite inclusions on crack growth is incorporated with a scalar factor into the crack growth law. Both models can describe the essential phenomena which are relevant for cast iron materials.

2. SYSTEM DEFINITION

The purpose of this section is to define Finite Element (FE) model of the engine assembly, key steps, engine parts, modeling techniques, and material model.

2.1. Engine Type And Components

The straight-six cylinder engine in Figure2.1 is used to perform this study.
The straight-six engine or inline-six engine (often abbreviated I6 or L6) is an internal combustion engine with the cylinders mounted in a straight line along the crankcase with all the pistons driving a common crankshaft. The bank of cylinders may be oriented at any angle, and where the bank is inclined to the vertical, the engine is sometimes called a slant-six. The straight-six layout is the simplest engine layout that possesses both primary and secondary mechanical engine balance, resulting in much less vibration than engines with fewer cylinders.[1]
The straight-six in diesel engine form with a much larger displacement is commonly used for industrial applications. These include various types of heavy equipment, power generation, as well as transit buses or coaches. Virtually every heavy duty over-the-road truck employs an inline-six diesel engine, as well as most medium duty and many light duty diesel trucks. Its virtues are superior low-end torque, very long service life, smooth operation and dependability. On-highway vehicle operators look for straight-six diesels, which are smooth-operating and quiet. Likewise, off-highway applications such as tractors, marine engines, and electric generators need a motor that is rugged and powerful. In these applications, compactness is not as big a factor as in passenger cars. Reliability and maintainability are much more important concerns.

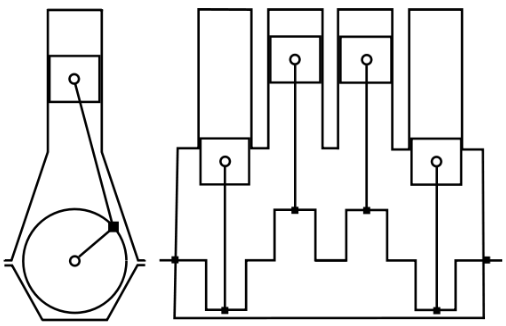

Figure 2.1: Straight engine model.

2.1.1. Cylinder head

In an internal combustion engine, the cylinder head (often informally abbreviated to just head) sits above the cylinders on top of the cylinder block. It closes in the top of the cylinder, forming the combustion chamber. This joint is sealed by a head gasket. In most engines, the head also provides space for the passages that feed air and fuel to the cylinder, and that allow the exhaust to escape. The head can also be a place to mount the valves, spark plugs, and fuel injectors.

In a flathead or sidevalve engine, the mechanical parts of the valve train are all contained within the block, and the head is essentially a metal plate bolted to the top of the block; this simplification avoids the use of moving parts in the head and eases manufacture and repair, and accounts for the flathead engine's early success in production automobiles. This design, however, requires the incoming air to flow through a convoluted path, which limits the ability of the engine to perform at high revolutions per minute (rpm), leading to the adoption of the overhead valve (OHV) head design, and the subsequent overhead camshaft (OHC) design.

2.1.2. Cylinder block

A cylinder block is an integrated structure comprising the cylinder(s) of a reciprocating engine and often some or all of their associated surrounding structures (coolant passages, intake and exhaust passages and ports, and crankcase). The term engine block is often used synonymously with "cylinder block" (although technically distinctions can be made between en bloc cylinders as a discrete unit versus engine block designs with yet more integration that comprise the crankcase as well).

In the basic terms of machine elements, the various main parts of an engine (such as cylinder(s), cylinder head(s), coolant passages, intake and exhaust passages, and crankcase) are conceptually distinct, and these concepts can all be instantiated as discrete pieces that are bolted together. Such construction was very widespread in the early decades of the commercialization of internal combustion engines (1880s to 1920s), and it is still sometimes used in certain applications where it remains advantageous (especially very large engines, but also some small engines). However, it is no longer the normal way of building most petrol engines and diesel engines, because for any given engine configuration, there are more efficient ways of designing for manufacture. These generally involve integrating multiple machine elements into one discrete part, and doing the making such as casting, stamping, and machining for multiple elements in one setup with one machine coordinate system of a machine tool or other piece of manufacturing machinery. This yields lower unit cost of production and/or maintenance and repair.

Today most engines for cars, trucks, buses, tractors, and so on are built with fairly highly integrated design, so the words "monobloc" and "en bloc" are seldom used in describing them; such construction is often implicit. Thus "engine block", "cylinder block", or simply "block" are the terms likely to be heard in the garage or on the street.

2.2. Data Requirements

2.2.1. CAD geometry

CAD geometry is required for the following components:

- Cylinder head, block, valve guides, valve inserts, head bolts, and gasket.

2.2.2. Material data

Temperature dependent thermal conductivity for the following components:

- Block, head, valve guide, valve inserts, bolts, and gasket.
  Non-temperature dependent values of density and Brinell hardness for the thermal conductivity calculations for: Head, valve guide and valve inserts.
- Temperature dependent values of Young's Modulus, Poisson's ratio and thermal expansion coefficient for the following components: Block, head, valve guide, valve inserts and bolts.
- Temperature dependent data is also required for the fatigue safety factor calculation on the block and head:

2.2.3. Thermal analysis data

- Coolant and oil bulk temperatures.
- CFD derived heat transfer coefficient distributions for water jackets.
- WAVE derived combustion gas cycle averaged temperature and heat transfer coefficients.

2.2.3. Structural analysis data

- Inlet and exhaust valve seat insert and guide interferences.

- Bolt loads and tightening procedure.
- Injector clamp loads.

A representative duty cycle for the failure rate calculation.

3. METHODOLOGY

3.1. Key Analysis Steps

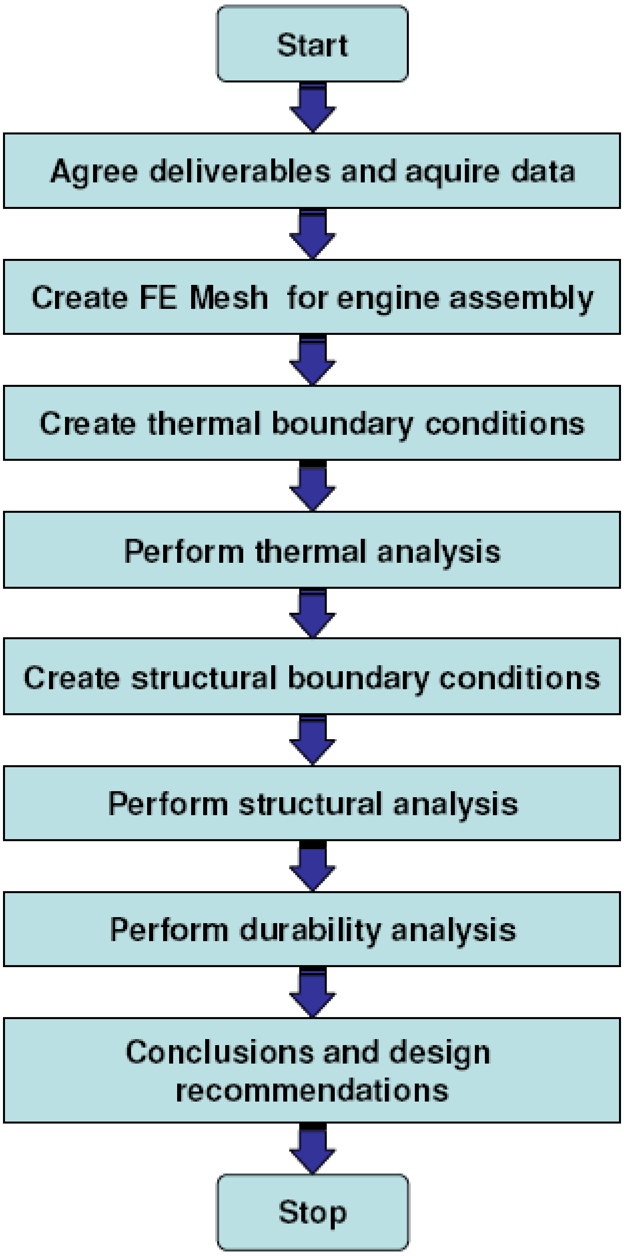

Figure 3.1: Key analysis steps.

The key analysis steps are illustrated in Figure 3.1 and described below:

- Acquire all input data, including geometry, material data and boundary conditions.

- Decide extent of engine model required for analysis (i.e. engine slice, bore and two halves or full engine).
- Generate appropriate finite element models of block,
- Ensure parabolic tetrahedral mesh passes ABAQUS data check
- Create conduction paths between components (i.e. valve to guide, head to gasket etc.)
- Create convection loading boundary conditions on model (i.e. combustion gases, oil and coolant).
- Linearise the FE mesh and create thermal deck.
- Solve for temperature distributions.
- Post process thermal results and evaluate temperatures against known acceptance criteria.
- Create a structural FE model by removing valves and thermal boundary conditions.
- Couple assemblies in an appropriate way (e.g. contact surfaces).
- Model structural boundary conditions (e.g. bolt load, firing pressure and restraints).
- Create structural deck with parabolic elements.
- Apply thermal load from solved temperatures.
- Solve for displacement and stress.
- Post process for valve misalignment, bore distortion, gasket sealing.
- Perform a simple fatigue safety factor durability assessment.
- Complete a more detailed fatigue evaluation against an agreed duty cycle.

3.1.1. Part orientation

- Set units to be SI and import geometry of the cylinder head, block, inserts, guides, valves, gasket and cylinder head bolts.
- Position and align the solid models to form an assembly.
- Re-orientate the assembly to the Ford engine co-ordinate system, as shown in Figure 3.2
- X-axis aligned to centre line of the crankshaft, pointing from front of engine to the rear
- Direction of Z-axis aligned to the centreline of bore 1
- Position the origin to align to the front face of the block

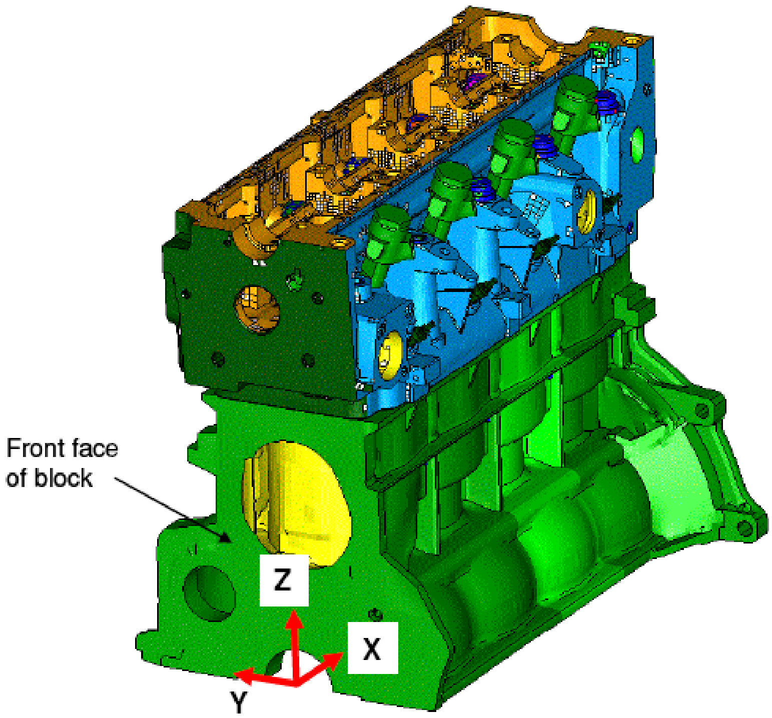

Figure 3.2 : Part orientation.

3.1.2. Creating FEM for multiple components

- A single FE model is created for each unique valve seat, valve guides and head bolts.
- The FEMs are copied for multiple instances and moved to correct position in the engine assembly, as shown in Figure 3.3

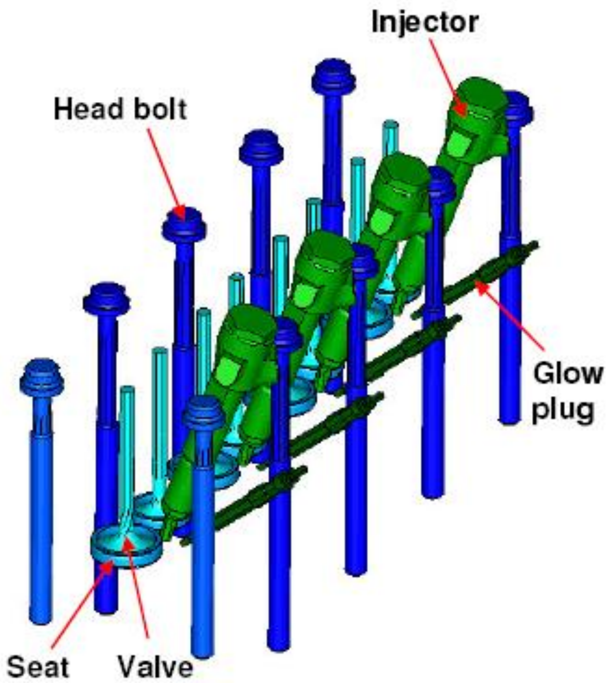

Figure 3.3 : Multiple instances of valve, seat, injector, glow plug and head bolt.

3.2. Meshing Of Cylinder Head And Block

It is aimed to preparing a durable mesh model, which will be used for structural analysis purposes, some critical parameters and meshing requirements are included in this document as a meshing guideline. Valve seats and valve guides are explained together with a detailed head meshing guide. Although this guideline is specific to meet head meshing requirements it is also useful for modeling other components and for other similar analysis types.

In general first order hexagonal elements or second order tetragonal elements are preferred to use for coupled thermo-structural analysis. And also it is a known fact that first order Hex elements are preferred due to their less computation time need and more accuracy on contact surfaces. In this procedure it is aimed to use first order tetra elements formed by surface elements (1st order trias). Tetra elements are used instead of hexa elements since the model geometry is complicated and there is no severe problematic area of contact. The main reason of meshing tria elements first is to generate tetra elements which are controlled by the surface elements and with more satisfied quality check outputs. Mesh model should consist of head mesh, valve guides and valve seats.

Table 3.1 : Element quality check parameters. [1]

Entities	2-D (tria)	3-D (tetra)
Warpage	5/40(min)	5/40
Aspect Ratio	5	5
Skew	60	60
Chord. Dev.	0.1	
Jacobian	0.5	0.5
Length	-	-
Taper	0.5	-
Min. Angle	45/20	20/5
Max. Angle	120/160	120/160
Tetra Collapse	-	0.1
Volume Skew	-	1
Volume A.R.	-	5

Cylinder Head Tetra Meshing Requirements, as shown in Table3.1

- Cylinder Head model for 3 cylinders.
- Number of nodes (second order tetra) including valve seats and valve guides<650.000
- Number of elements < 370.000

Mesh Requirements (tria):

- There should be no free edges.
- No duplicate elements.
- No self interference.
- No T-connections.
- Element normals should be consistent.
- No thin walled areas.
- Elements with extremely small size should be avoided.

Mesh Requirements (tetra):

- Element properties should follow element quality check criterions
- Check if your elements belong to correct components.
- Check material properties and element properties assigned to the elements.
- Minimum element interior angle>10 degree.
- Maximum element interior angle<145 degree.
- For second order tetra mesh the position of midside nodes and element jacobian should be controlled.

Mesh Density:

- 2 mm around the critical edges (combustion chamber
- At least 40 elements should be situated around the valve seats distributed on 360 degree.
- Element size should be 2-3 mm for the critical areas of the water jacket.
- For the other parts of the head the mesh size should be more than 8 mm in order to meet node and element amount limitations.
- The transition should be smooth through coarse elements to fine elements.
- In order to achieve smooth transition there should be a surface section as an offset from the hole, therefore the elements around the hole transfers smoothly.
- Mesh details of combustion chamber valve seats inserts and valve guides should be included.

Meshing requirement for analysis:

- For the valve seat model the necessary condition is to match the nodes of the seats with the head mesh exactly. This makes it more convenient to have proper contact between the valve seats and head.
- Elements and nodes of the guides which interfere with the head should be similar and exactly the same if it is possible. Since there will be an interference fit or negative clearance on the part surface.
- The shell elements should be organized properly as: combustion chamber, gasket, intake port, exhaust port, valve seats, valve guides, water jacket, oil channel, head surfaces and bolts.

- Mesh of the bottom part of the head should match the mesh of corresponding gasket mesh. This arrangement makes it more convenient to converge for contact interactions.
- Around the valve guide hole the mesh should be at least 10 elements.
- Bolt surfaces and bolt holes should be meshed at least 6 elements around bolt hole.

Lessons Learned

- For the ease of convergence and modeling purposes if it is possible mesh of the valve seats, valve guides and gasket should be same as the corresponding mesh area of the head component.
- Auto-clean up option should be avoided to use for head mesh.
- Mesh density for the water jacket should be fine (2mm or at least 4 elements) for the narrow region between intake and exhaust port.
- To have smooth transition between fine and coarse mesh pattern, the surface geometry of the model should be prepared with care and there should be at least 2 separate surface sections around the critical hole regions.
- Right angled tetra elements should be used for bolt holes to avoid
- Engine model could be cut in to sections. At first the cutting plane between the cylinder holes should be formed. And surfaces should be cut among this plane section. Different ID numbers should be given to the head sections and the corresponding components. Surfaces should be kept in the model together with surface mesh.

Finite element model is shown in Figure3.4 to Figure3.8

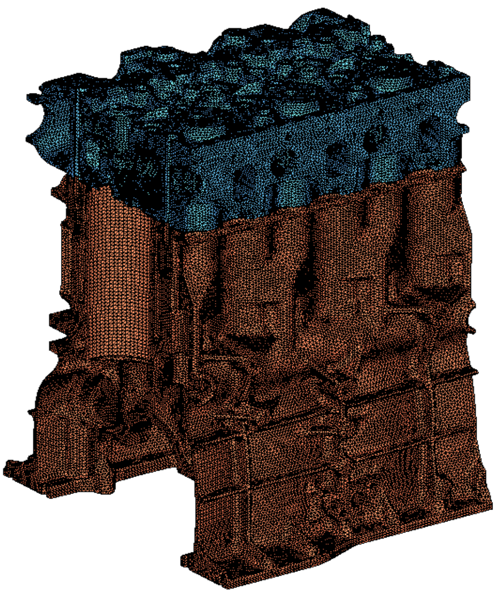

Figure 3.4 : Finite element model of the engine.

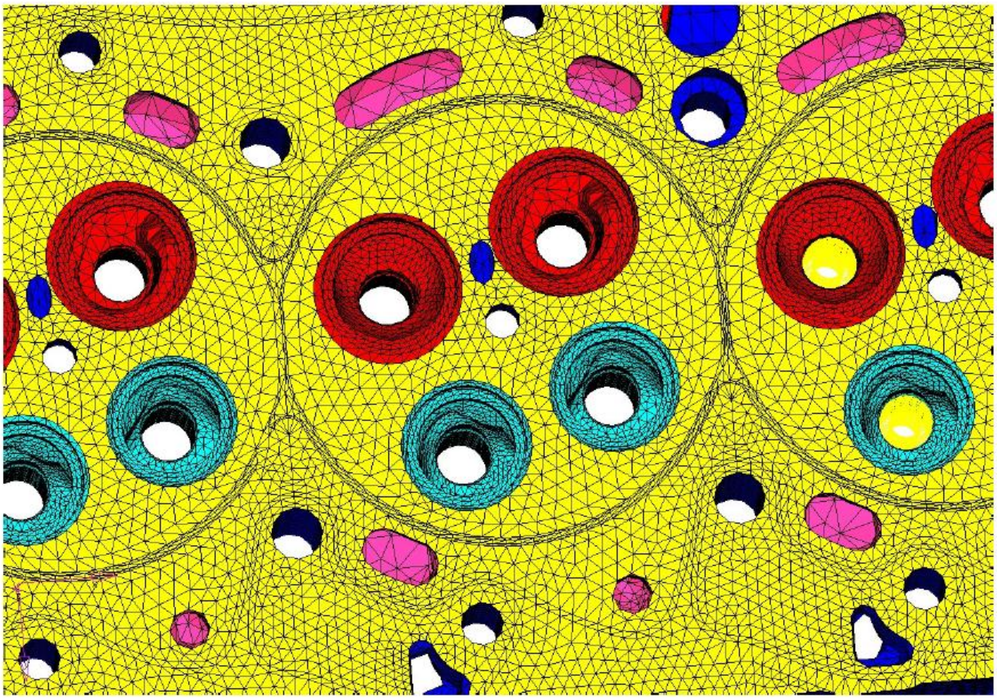

Figure 3.5 : Mesh density for the bottom of the head.

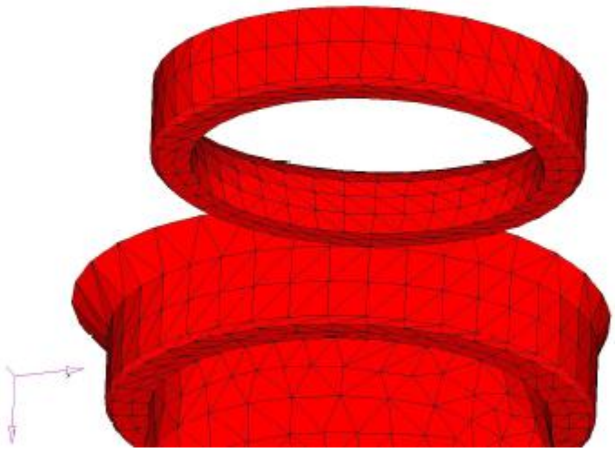

Figure 3.6 : Mesh of the valve seats and exhaust port.

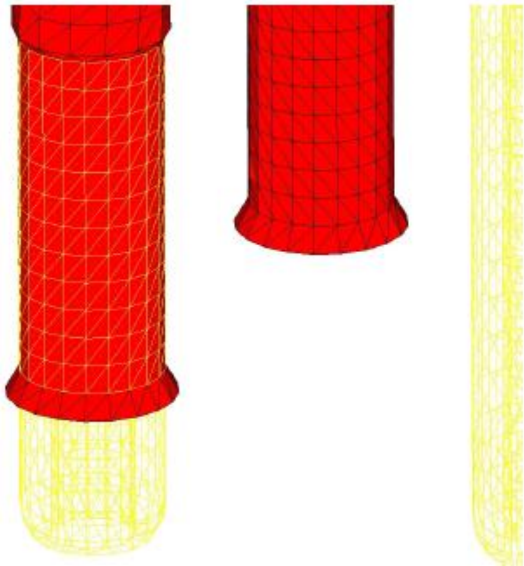

Figure 3.7 : Valve guide models (mesh exactly meets with head mesh).

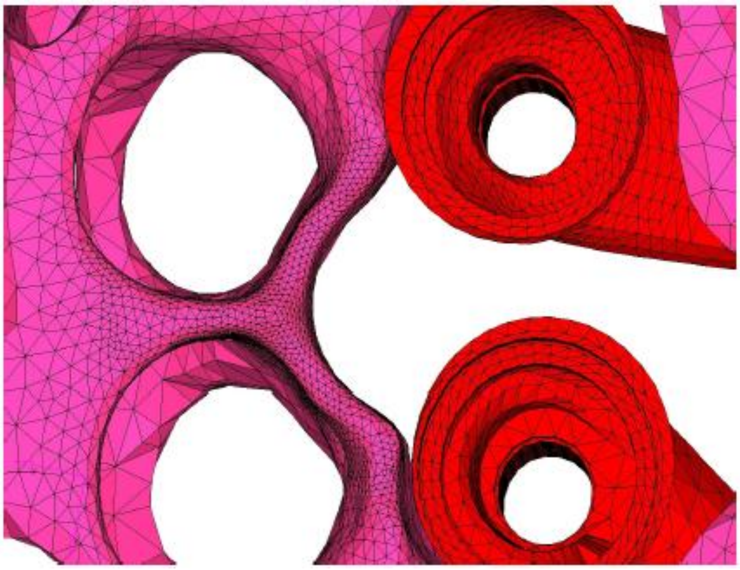

Figure 3.8 : Mesh density for the critical areas on the water jacket.

3.3. Sub-Modelling

Sub-modeling allows the analyst to focus on a subset of a model based on an existing solution from a global model. For example, sub-modeling can be used to perform a detailed analysis of a cylinder head display based on the results of a structural analysis.

An initial global analysis of a structure usually identifies critical regions.

Sub-modeling provides an easy modeling enhancement of these areas without having to resort to re meshing and reanalyzing the entire model.

Sub-modeling can reduce analysis costs while providing detailed results in local regions of interest.

- Use a coarse model to obtain the solution around the local region of interest.
- Use a refined mesh of the local region only for the local analysis.

Further refinement is possible if desired, since sub-modeling can be used through several levels;

- The local model for one level can be used as the global model for the next.

3.3.1 Sub-Modelling procedure

The steps of the sub-modeling procedure

- Obtain a global solution of the whole model (Figure3.9) using a level of mesh refinement that allows acceptable solution accuracy.
- Interpolate this solution onto the boundary of a locally refined mesh.
- Obtain a detailed solution in the local area of interest.
- The solution from the global model is interpolated automatically as needed to “drive” the displacements on the boundary of the local model.

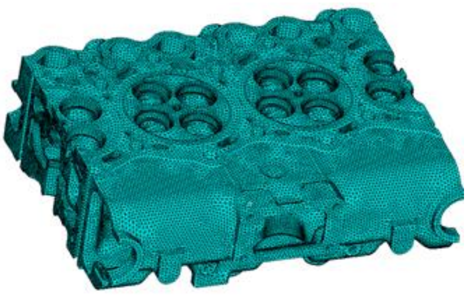

Figure 3.9 : Global cylinder head model.

Location of the sub-model boundary

- Deciding the actual location of the local boundary requires some engineering judgment.
- The sub-model boundary should be far enough away from the area of the sub-model where the response is changed by the different modeling.
- That is, the solution at the boundary should not be altered significantly by the different local modeling (Saint-Venant's Principle).

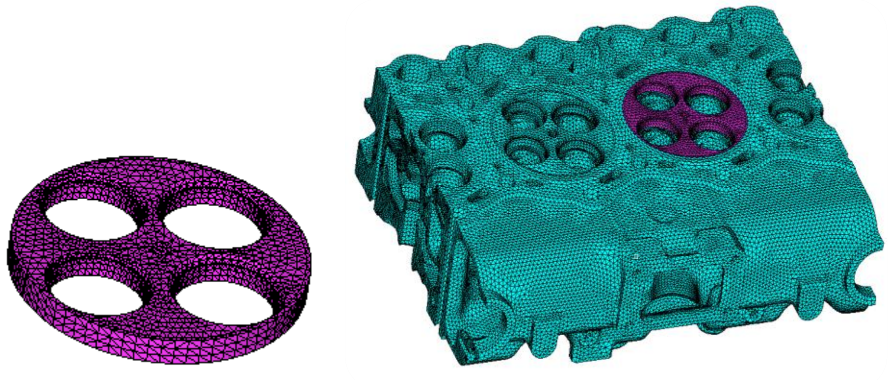

Figure 3.10 : Sub-model and orientation of sub-model into global model.

- Sub-modeling can be applied quite generally in ABAQUS as shown in Figure 3.10
- The material response defined for the sub-model may be different from that defined for the global model.
- The global and sub-model procedures do not have to be the same.
- For example, the nonlinear dynamic response of the global model can be used to drive the static, nonlinear response of the sub-model on the grounds that the sub-model is too small for dynamic effects to be significant in that local region.
- The global procedure can be performed in ABAQUS/Standard to drive a sub-modeling procedure in ABAQUS/Explicit and vice versa as shown in Figure 3.11
- For example, a static analysis performed in ABAQUS/Standard can drive a quasi-static ABAQUS/Explicit analysis in the sub-model.
- The step time used in the analyses can be different; the time variation of the driven nodes can be scaled to the step time used in the sub-model.

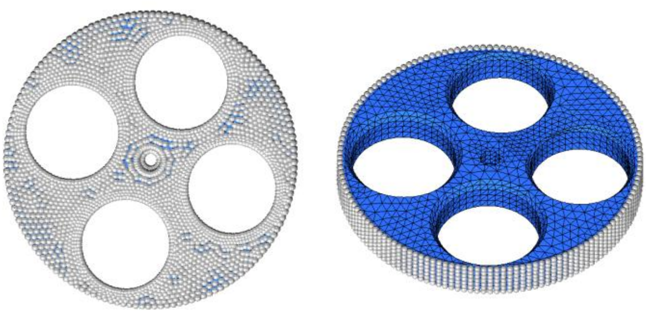

Figure 3.11 : Driven nodes on sub-model.

4. THERMAL ANALYSIS SET-UP

This section covers how to create the thermal boundary conditions on the FE model. Three modes of heat transfer exist: conduction, convection and radiation. Conduction is the heat transfer through solids and fluids at rest, due to a temperature gradient. Heat is transferred by conduction through the cylinder head, cylinder walls and valves; through the piston rings; through the block and manifolds. Conduction through a component is easily accounted by the inclusion of thermal conductivity within the material definition of an element. The diffuculty is to account for the conduction across a metal to metal boundary. Heat is transferred through fluids in motion and between a fluid and solid surface in relative motion. This form of heat transfer is called convection. When fluid motion is produced by forces other than gravity, the term forced convection is used. Heat transfer is occured by forced convection between the in-cylinder gases and the cylinder head, valves, cylinder walls and the piston. Simultaneously it is transferred by forced convection from the cylinder walls to the coolant and from the piston to the lubricant. Substantial convective heat transfer occurs to the exhaust valve, exhaust port and exhaust manifold during the exhaust process. The fluids available for this type of loading are the combustion gases, lubricating oils and coolant. How and where to apply convection boundary conditions are discussed in following sections. Heat exchange by radiation occurs through the emission and absorption of electromagnetic waves. Heat transfer by radiation occurs from the high temperature combustion gases and the flame region to the combustion chamber walls. Radiation is not explicitly included within the TMF model. The current TMF process does not covers thermal connection between the piston and the block liner.

4.1. Thermal Conduction

4.1.1. Creation of conduction paths

Thermal conductance typical occurs between the following components:

- Valve guide to cylinder head
- Valve Seat to cylinder head
- Head bolt to cylinder head
- Head bolt to cylinder block
- Cylinder head to gasket (stopper/bead/body)
- Gasket (stopper/bead/body) to cylinder block

Values of Thermal Contact Conductance

Thermal contact conductance between components is a complicated phenomenon, influenced by many factors. Experience shows that the most important ones are as follows:

- Contact pressure - as contact pressure grows, contact conductance grows.
- Surface quality – surface imperfections, cleanliness and deformation

The analytical equations have been found to estimate contact conductance using material properties, contact pressure and contact area. Typical values of conductance for the contact regions in the Diesel Engine are shown in Table 4.11

Table 4.1 : Element quality check parameters. [1]

Contact region	HTC / Wm^2K
Valve guide to cylinder head	2044
Valve stem to valve guide	2044
Valve to valve seat	2044
Valve seat to cylinder head	8177
Cylinder head to gasket stopper	10000
Cylinder block to gasket stopper	10000
Cylinder head to gasket body	10000
Cylinder block to gasket body	10000
Head bolt to cylinder head	10000

4.2. Thermal Convection

4.2.1 Creation of convection heat transfer regions

For each convective boundary condition, thin shell elements should be created on every element face that would experience that particular loading. Figure 4.1 to Figure 4.4 show typical regions for convective loading for the cylinder block, head and valve seats. The user should confirm the convective areas with component engineers as the region definitions will be different from engine to engine. The cylinder block experiences no combustion loading except the liner. Coolant side HTC generated from CFD analysis is generally mapped onto the water jacket. Generally some generic HTC values are applied to the oil room and oil rail.

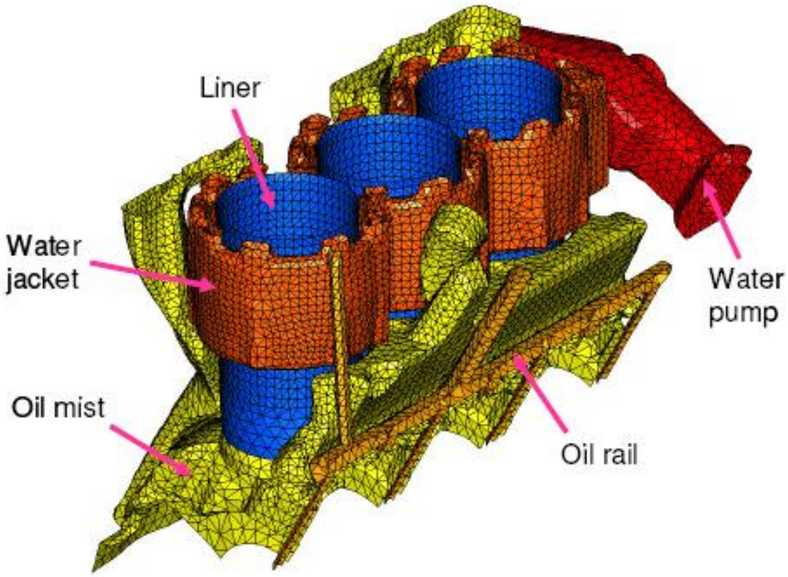

Figure 4.1 : Typical regions for convection loading on cylinder block.

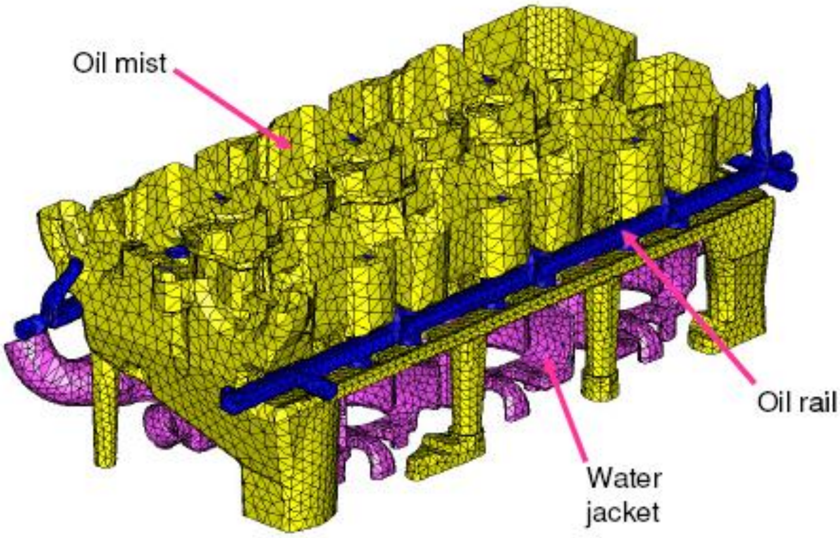

Figure 4.2 : Typical oil and water jacket regions in a cylinder head.

The combustion loadings are applied to the cylinder head, the valves and the valve seats. The division of the regions requires careful consideration. Figure 4.3 and Figure 4.4 provide a guideline illustration of the combustion loading areas. The extent of each area definition should be agreed with performance simulation engineers who supplies the gas side HTCs.

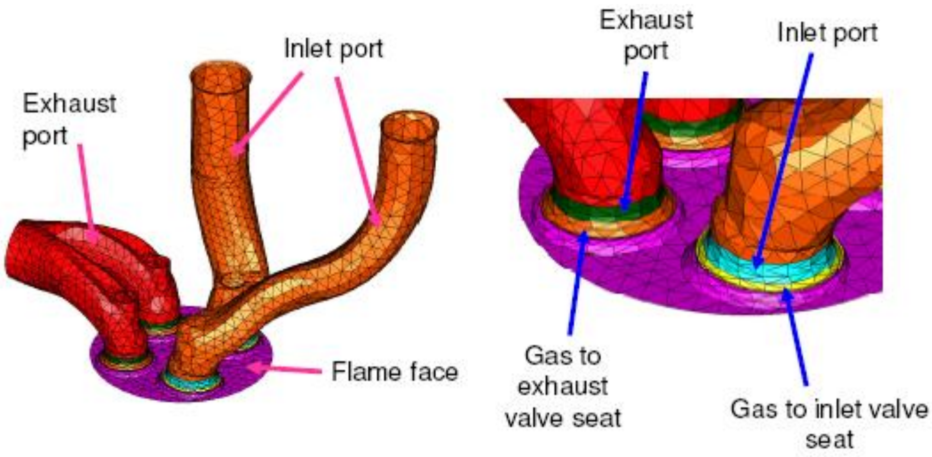

Figure 4.3 : Typical regions for combustion loading on head and seats.

4.2.2 Coolant side HTC

If available, HTCs derived from a CFD analysis can be applied in the coolant side, Figure 4.4 shows the comparison of the mapped HTCs to CFD results.

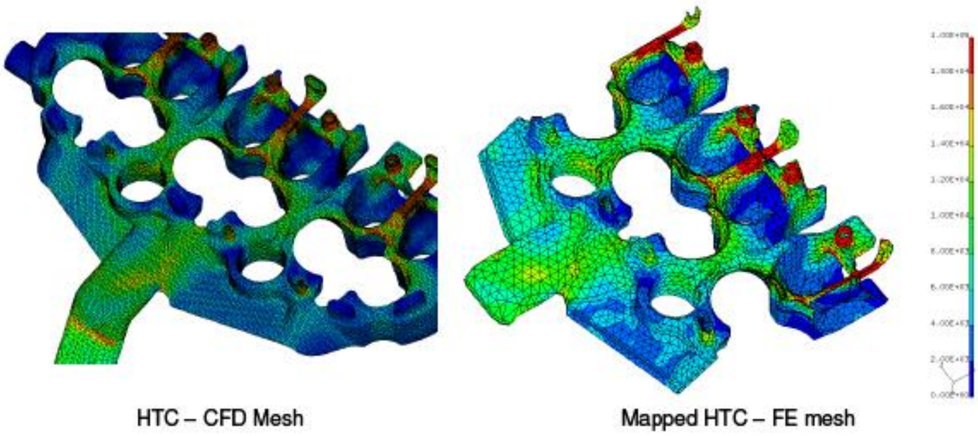

Figure 4.4 : Mapped HTC from CFD analysis.

5. STRUCTURAL ANALYSIS SET-UP

This section describes the structural boundary conditions required for a thermo-mechanical analysis. There are two types of non-linearity that can be included within the analysis: material and contact.

Examples of material non-linearity in a TMF model are:

- Non-linear stress-strain characteristics of cast iron and the cylinder head gasket
- Elastic-plastic characteristics of aluminium cylinder heads and block

Examples where contact is included within a TMF model are:

- At the interface between the cylinder head gasket with the cylinder head and block
- At the interface between the valve insert and head

Depending upon the scope of work either a fully linear analysis is performed or some nonlinearity is specified. This document excludes the modeling of material non-linearity.

Key Steps

The structural boundary conditions to be applied to a TMF model are:

- Rigid body motion of the model must be removed. Typically the interface of the bearing cap and block is restrained and any planes of symmetry or cut planes are included.
- Contact surfaces are used to couple the different components. Contact surfaces included are between the head/block and gasket, guides/inserts and head, and cylinder head bolt to head/block.
- Four types of loading are included within a TMF model. These are head bolt loads, injector clamping loads, and thermal loads.

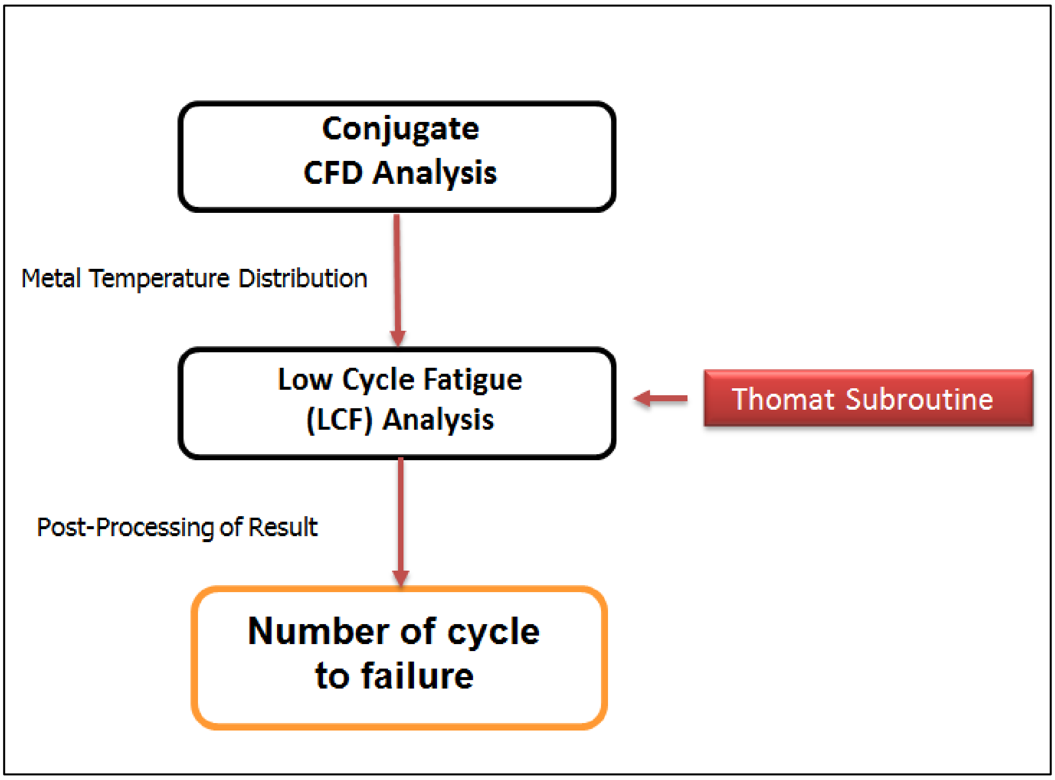

Figure 5.1 : Analysis flow chart.

Low-cycle fatigue (LCF) post-processor Thomat, an in-house software developed by Fraunhofer IWM, is used to determine LCF life based on structral FE results as shown in Figure 5.1

5.1. Coupling Components Into An Aassembly

5.1.1. Bolts / cylinder head coupling

The coupling between head bolts and cylinder head is achieved through the use of ABAQUS contact.

The following steps illustrate the coupling between head bolts to cylinder head:

1. Faces of the solid elements to be used in each contact region need to be identified, as shown in Figure 5.2

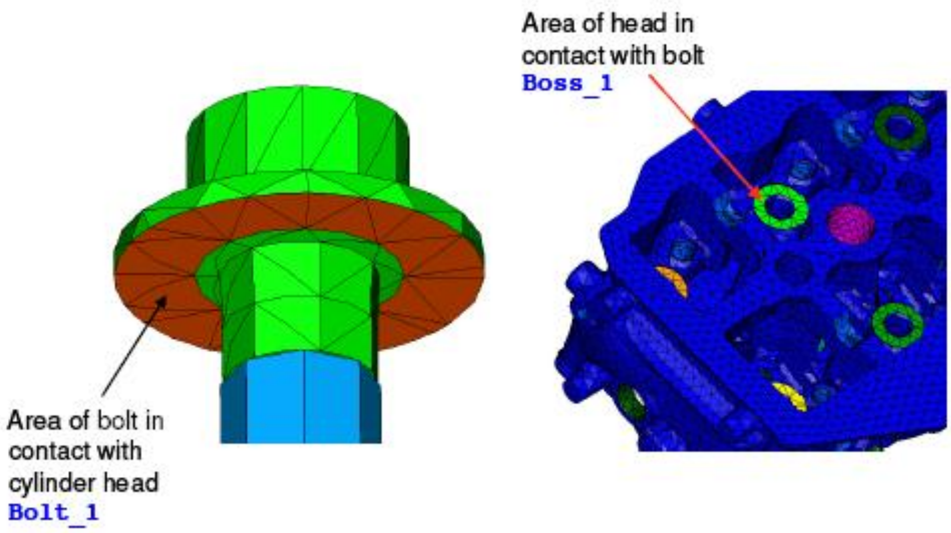

Figure 5.2 : Bolt and cylinder head contact pairs.

5.1.2. Cylinder head / gasket / block coupling

ABAQUS contact pairs are used to model the interaction between gasket elements and head/block.

1. Surfaces are defined on the top and bottom surfaces of the gasket elements, shown in Figure 5.3

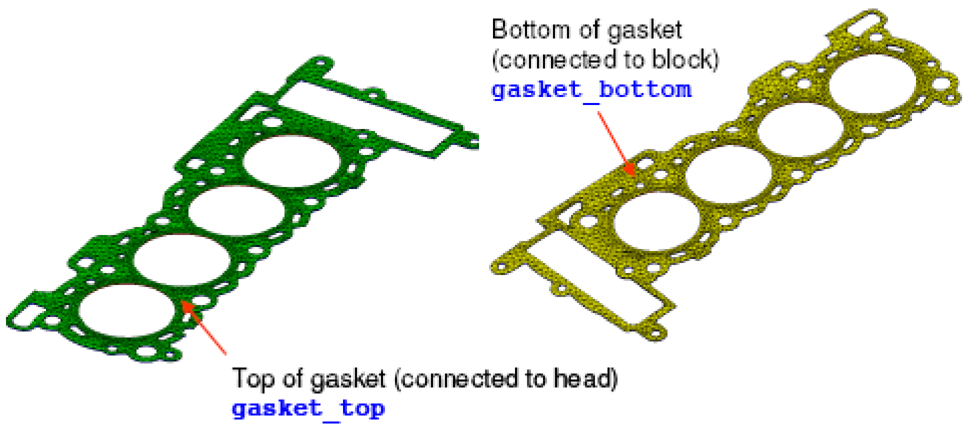

Figure 5.3 : Gasket contact surface definitions.

Respective contact surfaces to the gasket are also defined for the head and block, as shown in Figure 5.4

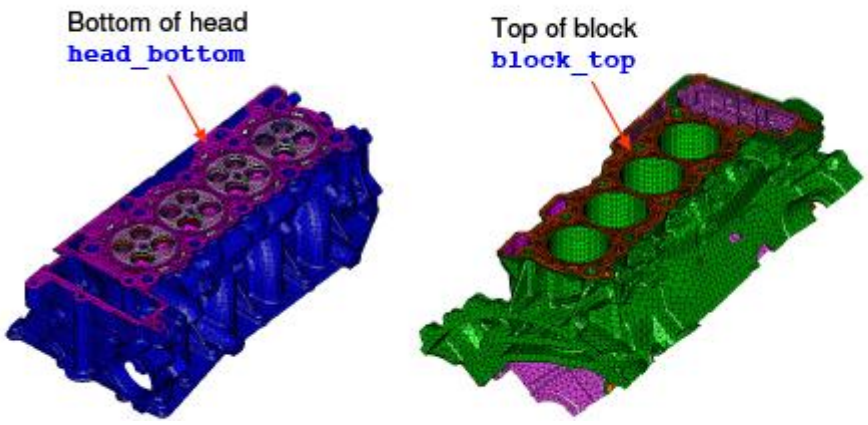

Figure 5.4 : Head and block contact surface definitions.

5.1.3. Valve guide and valve seat interference

Press fit of valve seats and guides generates significant stresses in the cylinder head, as shown in Figure5.5. ABAQUS is capable of computing the interference from initial coordinates. This process requires the precise specification of the nodal coordinates if the interference is small.

A more exact technique to specify precise over-closure of 32.5mm is described below for pressure fit of inlet valve seats.

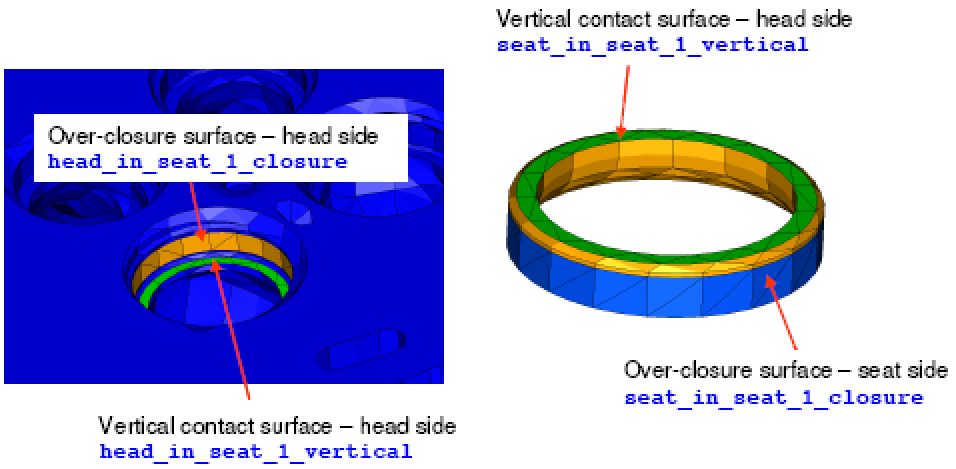

Figure 5.5 : Valve seat contact surfaces.

5.2. Restraints

The block should be restrained as far away from the area of interest (i.e. top of block and cylinder head) as possible. Typically the block is modeled as far down as the split line of the caps / bed plate. The split line is a good place to restrain the block, as it mimics the firing load on the head being reacted by the firing load transferred via the piston and con rod to the crankshaft.

Add restraints to the bottom of the block in order to prevent rigid body motion. The reaction should not be done at a single point, as this will lead to high stress and large displacements at the point.

5.2.1. Applied loads

In addition to the valve guide/seat interference in the cylinder head, the loads modelled in a typical structural analysis are bolt load, firing pressure, injector clamp and thermal load. A combination of these loads makes up the load cases from which the durability is assessed.

5.2.2. Bolt load

1. Note the element label of the middle beam element, as shown in Figure5.6.
2. Create a node at the centre of the bolt shank. Note the node label.

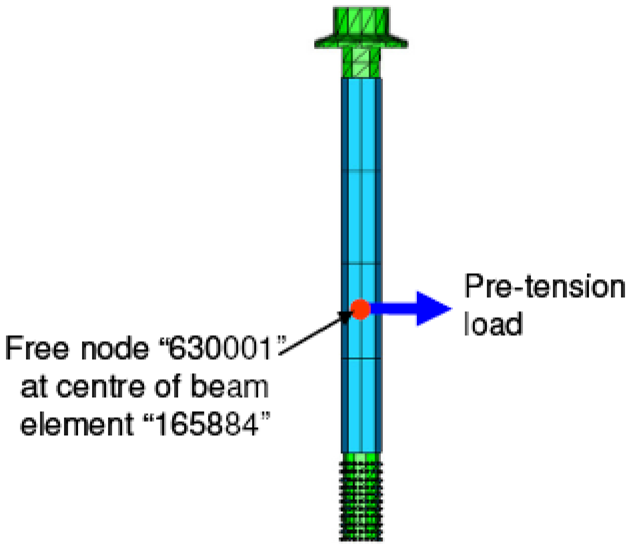

Figure 5.6 : Bolt load set-up.

3. Apply the bolt force in the x-direction to these nodes. The bolt load on this node is applied to the middle beam element of the bolt shank, via the *PRE-TENSION SECTION card:
   *PRE-TENSION SECTION,NODE=630001,ELEMENT=165884
4. The pre-tension load is specified using the *CLOAD card after the *STEP as part of boundary condition set-up:

```
*STEP, AMPLITUDE=RAMP,INC=10
*STATIC
*CLOAD, OP=NEW
630001, 1, 9.04E+04
```

5. After the first load step, a second load step is created so that this force is swapped for an enforced displacement, using the *BOUNDARY, FIXED command. By changing to an enforced displacement, the bolt force is allowed to vary in subsequent load cases.

```
*STEP, AMPLITUDE=RAMP,INC=10
*STATIC
*BOUNDARY, FIXED
BS000006, 1,
*CLOAD, OP=NEW
*END STEP
```

5.2.3. Thermal load

After an ABAQUS thermal analysis has been completed, the following capability within ABAQUS can be used to read the thermal analysis results file and impose them onto the structural model.

1. Put the ABAQUS results file into the working directory and include the following parameter in the history definition of the ABAQUS deck:

```
*TEMPERATURE, MIDSIDE, FILE = <thermal_results_file_name>
```

2. ABAQUS will calculate the temperatures at the mid-side nodes of the second-order elements using the corner node values.

5.2.4. Injector clamp load

The injector is clamped to the cylinder head by two bolts. *PRE-TENSION section is used in the bolts to apply the load.

The injector body is a solid mesh. The elements and nodes at the base are matched to cylinder head to avoid using a contact surface, which will increase CPU time. The set-up is shown in Figure 5.7

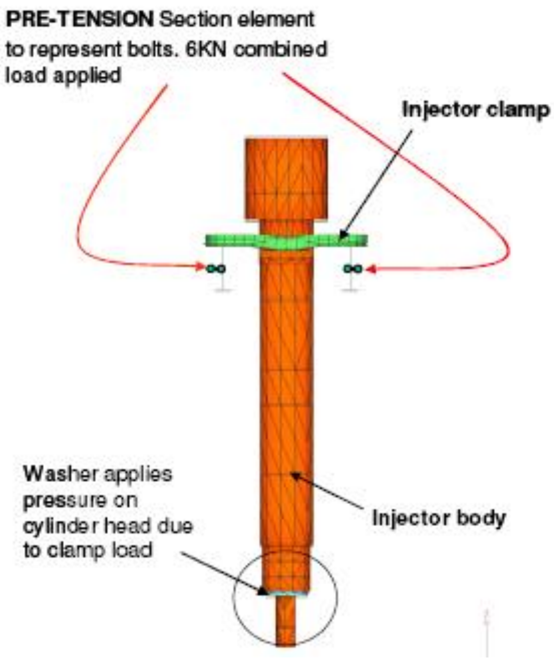

Figure 5.7 : Injector load set-up.

5.3. Analysis Step Definition

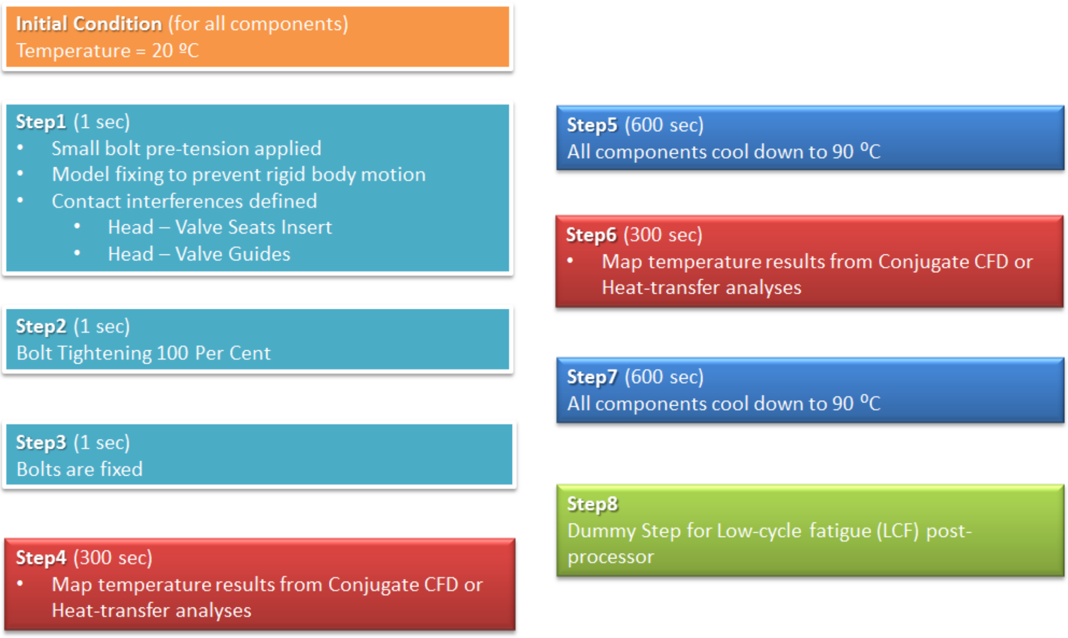

Figure 5.8 : Structural analysis step definition.

Firstly, all model components' temperature is set to 20 ^{o}C, this is initial condition for our system, as shown in Figure5.8.

```
*INITIAL CONDITIONS, TYPE = TEMPERATURE
NALL,20.
```

5.3.1. Mechanical loading steps

STEP1**,** Mechanical loadings are defined at this step. As defined in Section 5.2, Structural model is fixed to prevent rigid body motion from main cap bearings at cylinder block component. Contact interferences defined between Cylinder Head-Valve Seat Inserts and Cylinder Head-Valve Guides. And Finally, Small pretension load is applied to all bolts.

```
*STEP, INC =          200
PRESS FIT & SMALL BOLT PRETENSION
*STATIC
0.4       ,1.0       ,          ,
*BOUNDARY, OP=NEW
nfx123,1,3,0.0
nfx12,1,2,0.0
nfx2,2, ,0.0
*CLOAD
boltf,1,1000.0
*CONTACT INTERFERENCE, SHRINK, TYPE = CONTACT PAIR
hvins1s, vins1s
hvins2s, vins2s
hvins3s, vins3s
hvins4s, vins4s
hvexs1s, vexs1s
hvexs2s, vexs2s
hvexs3s, vexs3s
hvexs4s, vexs4s
h_v_g_1, v_guide_1
h_v_g_2, v_guide_2
h_v_g_3, v_guide_3
h_v_g_4, v_guide_4
h_v_g_5, v_guide_5
h_v_g_6, v_guide_6
h_v_g_7, v_guide_7
h_v_g_8, v_guide_8
h_v_g_9, v_guide_9
h_v_g_10, v_guide_10
h_v_g_11, v_guide_11
h_v_g_12, v_guide_12
*CONTACT CONTROLS, STABILIZE
*EL FILE, ELSET = Headall, FREQUENCY = 999, POSITION = AVERAGED AT
NODES
```

```
S,
*OUTPUT, FIELD, FREQUENCY = 999
*NODE OUTPUT
U,
*ELEMENT OUTPUT
S,
*OUTPUT, FIELD, FREQUENCY = 999
*ELEMENT OUTPUT, ELSET = Headall
PEEQ,
*END STEP
```

STEP2, Full load is applied to all bolts.

```
*STEP, INC =        200
BOLT TIGHTENING 100 PER CENT
*STATIC
0.4     ,1.0     ,        ,
*CLOAD
boltf,1,175000.0
*CONTACT CONTROLS, STABILIZE
*END STEP
```

STEP3, Bots are fixed to prevent to loose connection.

```
*STEP, INC =        200
FIXED BOLT LOAD B.C.
*STATIC
1.0     ,1.0     ,        ,
*BOUNDARY, FIXED
boltf,1, ,0.0
*END STEP
```

5.3.2. Thermal Loading Steps

STEP4 & STEP6, These are Heat-Up steps. Temperature results from conjugate CFD analysis are mapped on the structural analysis.

```
*Step, INC=1000
heat_up1
*Static
5., 30., 1e-05, 10.
*INCLUDE, INPUT =EU5_thermal_400ps_18102011.inp
*OUTPUT, FIELD, FREQUENCY=999
*EL FILE, ELSET = Head, FREQUENCY = 999, POSITION = AVERAGED AT
NODES
S,
*OUTPUT, FIELD, FREQUENCY = 999
*NODE OUTPUT
U,
NT,
```

```
*ELEMENT OUTPUTS,
*OUTPUT, FIELD, FREQUENCY = 999
*ELEMENT OUTPUT, ELSET = Head
PEEQ,
*END STEP
```

STEP5 & STEP7, These are Cool-Down Steps. All components temperature values are set to 90 ^{o}C. This value is taken from test data. When engine working at idle condition all components temperature's nearly 90^{o}C.

```
*Step, INC=1000
cool_down1
*Static
5., 60., 1e-05, 20.
*TEMPERATURE , OP=NEW
NALL,90
*EL FILE, ELSET = Head, FREQUENCY = 999, POSITION = AVERAGED AT
NODES
S,
*OUTPUT, FIELD, FREQUENCY = 999
*NODE OUTPUT
U,
NT,
*ELEMENT OUTPUT
S,
*OUTPUT, FIELD, FREQUENCY = 999
*ELEMENT OUTPUT, ELSET = Head
PEEQ,
*END STEP
```

STEP8, This is a dummy step for Thomat Subroutine to calculate faiulure cycle value.

```
*STEP, INC=1000
*STATIC
0.99, 0.99, 0.00001, 0.99
*OUTPUT, FIELD, FREQUENCY = 999
*ELEMENT OUTPUT, Elset=Headall, POSITION=INTEGRATION POINTS
SDV45
SDV46
SDV47
*END STEP
```

5.4. Thermo-Mechanical Cycle Definition

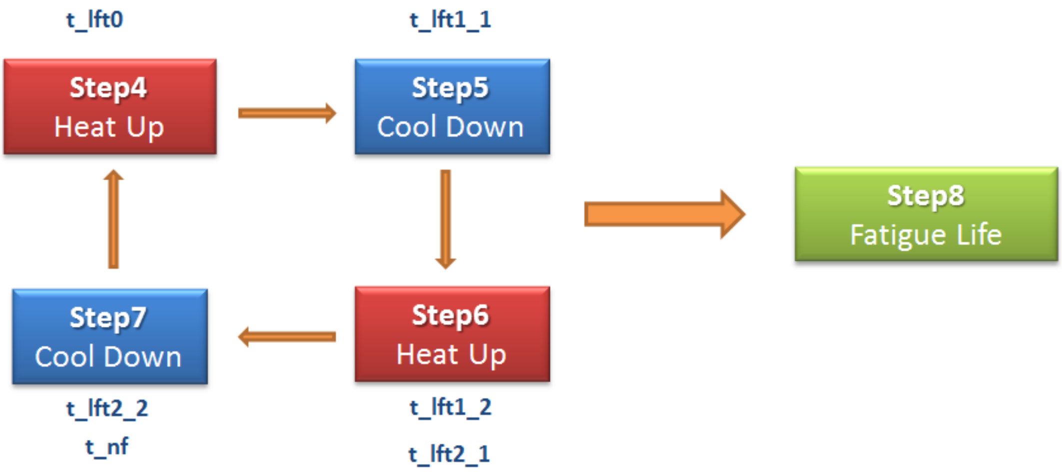

Figure 5.9 : Thermo-mechanical cycle definition. [9]

5.4.1. TMF Time Parameter

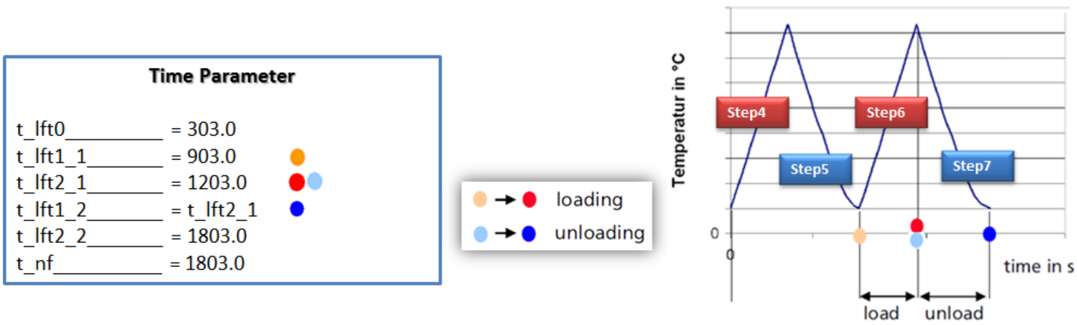

Figure 5.10 : TMF analysis time parameter. [9]

6. MATERIAL DEFINITION

CGI450 (Compacted Graphite Iron) is used both cylinder head and block.

6.1. Compacted Graphite Iron

As the demand for high torque, low emissions and improved fuel economy continues to grow, engine designers are forced to seek stronger materials for engine block construction. This is particularly true in the diesel sector where resolution of the conflicting performance objectives requires increased cylinder bore pressures. The bore pressures in today's direct injection diesels hover around 135 bar while the next generation of DI diesels are targeting 160 bar and beyond. Peak combustion pressures in heavy duty truck applications are already exceeding 200 bar, as shown in Figure6.1 At these operating levels, the strength, stiffness and fatigue properties of grey cast iron and the common aluminum alloys may not be sufficient to satisfy performance, packaging and durability criteria. Several automotive OEM's have therefore evaluated Compacted Graphite Iron (CGI) for their petrol and diesel cylinder block and head applications. Although compacted graphite iron has been known for more than forty years, and several review papers have been published, the properties of CGI are not yet as well-known as those of grey cast iron and the common aluminum alloys. This paper therefore provides more detailed information on the mechanical and physical properties of CGI as a function of the graphite nodularity, carbon content and the influence of ferrite and pearlite. The data presented are primarily from tests conducted at independent laboratories, although literature data is included and referenced where appropriate.

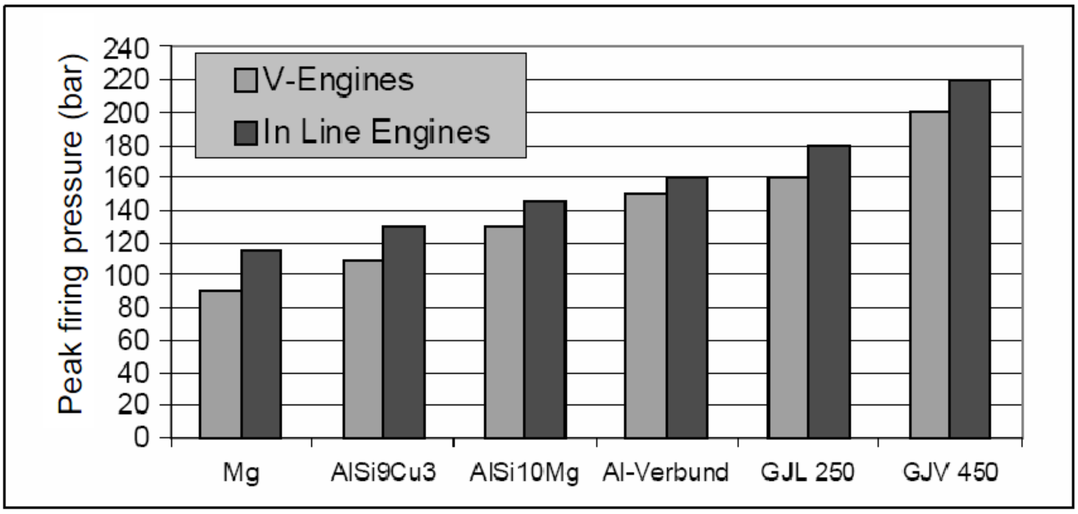

Figure 6.1 : Peak firing pressure limits for various materials in diesel engine cylinder block. [10]

Although Compacted (vermicular) Graphite Iron was first observed in 1948, the narrow range for stable foundry production precluded the high volume application of CGI to complex components such as cylinder blocks and heads until advanced process control technologies became available. This, in turn, had to await the advent of modern measurement electronics and computer processors. Following the development of foundry techniques and manufacturing solutions, primarily initiated in Europe during the 1990's, the first series production of CGI cylinder blocks began during 1999. Today, more than 40,000 CGI cylinder blocks are produced each month for OEMs including Audi, DAF, Ford, Hyundai, MAN, Mercedes, PSA, Volkswagen and Volvo.

Emissions legislation and the demand for higher specific performance from smaller engine packages continue to drive the development of diesel engine technology. While higher Pmax provides improved combustion, performance and refinement, the resulting increases in thermal and mechanical loads require new design solutions. Design engineers must choose between increasing the section size and weight of conventional grey iron and aluminium components or adopting a stronger material, specifically, CGI.

Given that new engine programs are typically intended to support three to four vehicle generations, the chosen engine materials must satisfy current design criteria and also provide the potential for future performance upgrades, without changing the overall block architecture. With at least 75% increase in ultimate tensile strength, 40% increase in elastic modulus and approximately double the fatigue strength of either grey iron and aluminium, CGI is ideally suited to meet the current and future requirements of engine design and performance.

6.1.1. Microstructure and properties

As shown in Figure 6.2, the graphite phase in Compacted Graphite Iron appears as individual 'worm-shaped' or vermicular particles.

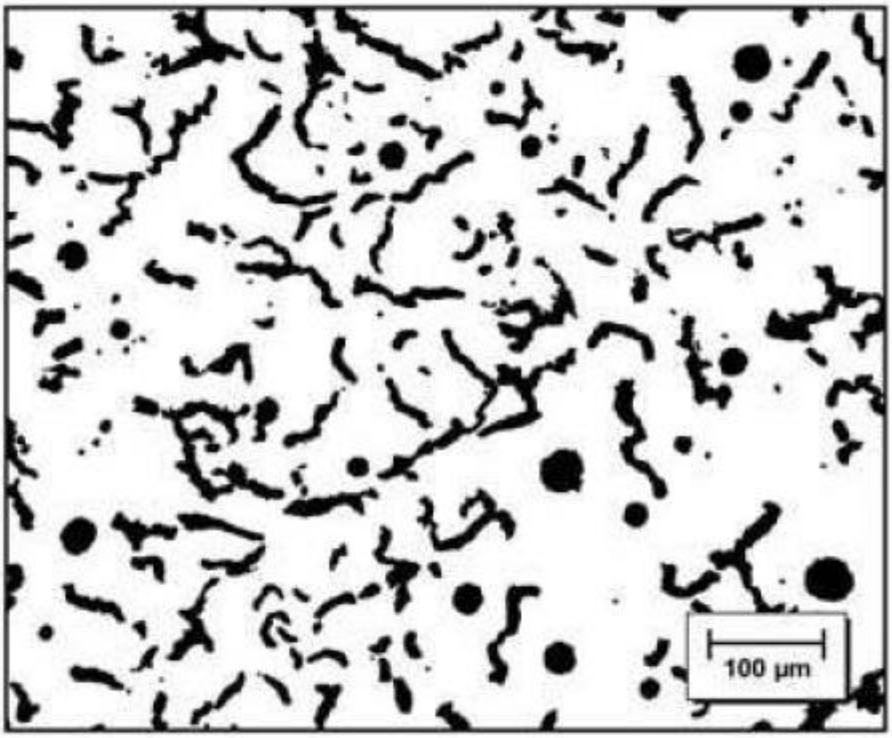

Figure 6.2 : CGI microstructure containing 10% nodularity. [2]

The particles are elongated and randomly oriented as in grey iron, however they are shorter and thicker, and have rounded edges. While the compacted graphite particles appear worm-shaped when viewed in two dimensions, deep-etched scanning electron micrographs (Fig. 6.3) show that the individual 'worms' are connected to their nearest neighbours within the eutectic cell.

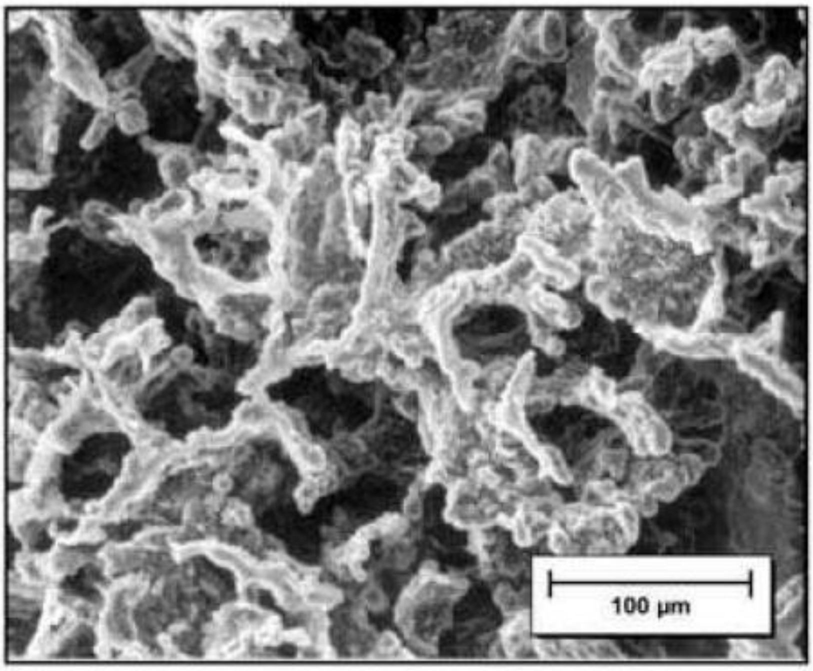

Figure 6.3 : Deep-etched SEM micrographs show the 3-D coral-like graphite morphology. [2]

The complex coral-like graphite morphology, together with the rounded edges and irregular bumpy surfaces of the compacted graphite particles, results in stronger adhesion between the graphite and the iron matrix, inhibiting crack initiation and providing superior mechanical properties

Compacted Graphite Iron invariably includes some nodular (spheroidal) graphite particles. As the nodularity increases, the strength and stiffness also increase, but only at the expense of castability, machinability and thermal conductivity. The microstructure specification must therefore be chosen depending on both the production requirements and the performance conditions of the product. In the case of cylinder blocks and heads, where castability, machinability and heat transfer are all of paramount importance, it is necessary to impose a more narrow specification. A typical specification for a CGI cylinder block or head can be summarised as follows:

- 0-20% nodularity, for optimal castability, machinability and heat transfer
- No free flake graphite, flake type graphite (as in grey iron) causes local weakness
- >90% pearlite, to provide high strength and consistent properties
- <0.02% titanium, for optimal machinability

This general specification will result in a minimum-measured tensile strength of 450 MPa in a 25 mm diameter test bar, and will satisfy the ISO 16112 Compacted Graphite Iron standard for Grade GJV 450. The typical mechanical properties for this CGI Grade, in comparison to conventional grey cast iron and aluminum are summarized in Table 6.1.

Table 6.1 : Mechanical and physical properties of CGI in comparison to conventional grey cast iron and aluminum at 20ºC. [2]

Property	Units	GJV 450	A 390.0
Ultimate Tensile Strength	MPa	450	275
Elastic Modulus	GPa	145	80
Elongation	%	1-2	1
Rotating-Bending Fatigue 20°C)	MPa	210	100
Rotating-Bending Fatigue (225°C)	MPa	205	35
Thermal Conductivity	W/m-K	36	130
Thermal Expansion	µm-m-K	12	18
Density	g/cc	7.1	2.7
Brinnell Hardness	BHN 10-3000	215-255	110-150

In Figure 6.4 it is compared Gray Iron, CGI and AlSi9Cu related to important properties for cylinder blocks and cylinder heads (Bick, 2003). It can be seen the low density and high thermal conductivity of aluminum alloys, the main reasons for the use of aluminum in cylinder heads.

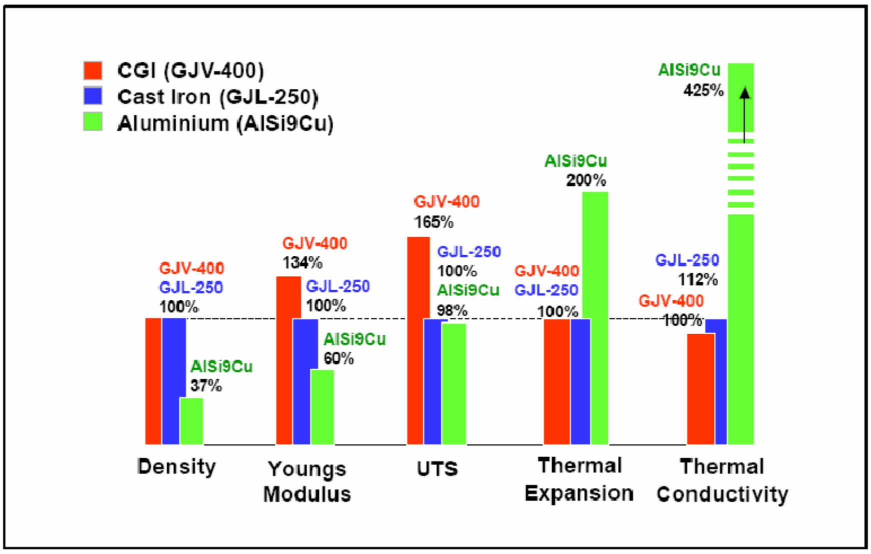

Figure 6.4 : Material properties, comparing CGI 400, Gray Iron 250 and AlSi9Cu. [11]

6.1.2. Engine design opportunities

Relative to conventional grey cast iron, CGI provides opportunities for:

- Reduced wall thicknesses at current operating loads
- Increased operating loads at current design
- Reduced safety factors due to less variation in as-cast properties
- Reduced cylinder bore distortion
- Improved NVH
- Shorter thread engagement depth and therefore shorter bolts

During the initial development period in the mid-1990's, much of the CGI development activity was focused on weight reduction. The data in Table 3 provide a summary of weight reduction results obtained in design studies conducted by various foundries and OEMs. The percent weight reduction values in parentheses refer to CGI cylinder blocks that are currently in series production and were published by the OEM. Although these cylinder blocks were never produced in grey iron (weight therefore presented as "xx.x"), the OEM stated that extra mass would have been required to satisfy durability requirements if the blocks were produced in conventional grey iron. While comparisons of the weight reduction potential depend on the size and weight of the original block, a weight reduction of 10-15% is a reasonable target for any CGI conversion program.

Since the introduction of common rail fuel injection, the emphasis in CGI engine development has shifted from weight reduction toward downsizing and increased power density. In this regard, the doubling of fatigue strength relative to grey iron and aluminum allow for significant increases in engine loading. One specific OEM study has shown that a 1.3 litre CGI engine package can provide the same performance as a current 1.8 litre grey iron engine. To achieve this increase, the Pmax was increased by 30% while the cylinder block weight was decreased by 22%. Despite the increase in Pmax, test rig fatigue analyses showed that the weight reduced CGI cylinder block provided a larger safety margin that the original grey iron block, thus indicating that further increases in performance were possible. In comparison to the original engine, the fully assembled CGI engine was 13% shorter, 5% lower, 5% narrower, and 9.4% lighter. This example demonstrates the contribution of CGI to achieve combined downsizing and power-up objectives.

Another consideration of CGI engine design is the ability to withstand cylinder bore distortion. In the combined presence of elevated temperatures and increased combustion pressures, cylinder bores tend to expand elastically. However, the increased strength and stiffness of CGI is better able to withstand these forces and maintain the original bore size and shape. The reduced cylinder bore distortion allows for reduced ring tension and thus reduced friction losses. Additional benefits include reduced piston slap thus improving NVH; reduced oil consumption thus extending oil change intervals; and, reduced blow-by thus preventing torque loss and improving emissions. Table 4 shows comparative bore distortion results for four grey iron and CGI engines with the same design.

The increased stiffness of CGI also contributes to NVH performance. Although the specific damping capacity of CGI is lower than that of grey iron, the higher elastic modulus stiffens the block, making many webs and ribs redundant. The 40% increase in the elastic modulus of CGI increases the separation between the combustion firing frequency and the resonant frequencies of the block. The net result of this increased separation is that the engine operation becomes quieter.

6.1.3. Thermal conductivity

The thermal conductivity of the graphite phase in cast irons is three to five times greater than that of either ferrite or pearlite [40]. It is therefore intuitively evident that the amount and shape of graphite are the critical factors in defining the thermal conductivity of cast irons. In order to quantify the effects of carbon content (in the practical CGI range of 3.5-3.8%), graphite shape, matrix composition and temperature on thermal conductivity, a series of controlled tests were conducted at the Austrian Foundry Institute (Österreichisches Giesserei-Institut, Leoben). The composition of the specimens, the test technique and the results are presented in this section.

The trends revealed in each of Figure 6.5 (a) through 6.5 (d) show that the thermal conductivity of CGI is approximately 25% less than that of pearlitic grey iron at room temperature and 15-20% less at 400oC. The thermal conductivity of grey iron decreases with increasing temperature is well known. However, even the presence of relatively small amounts of flake graphite in a predominantly compacted graphite microstructure also causes the conductivity to decrease with temperature. In contrast, the thermal conductivity of CGI and nodular cast irons gradually increases with increasing temperature.

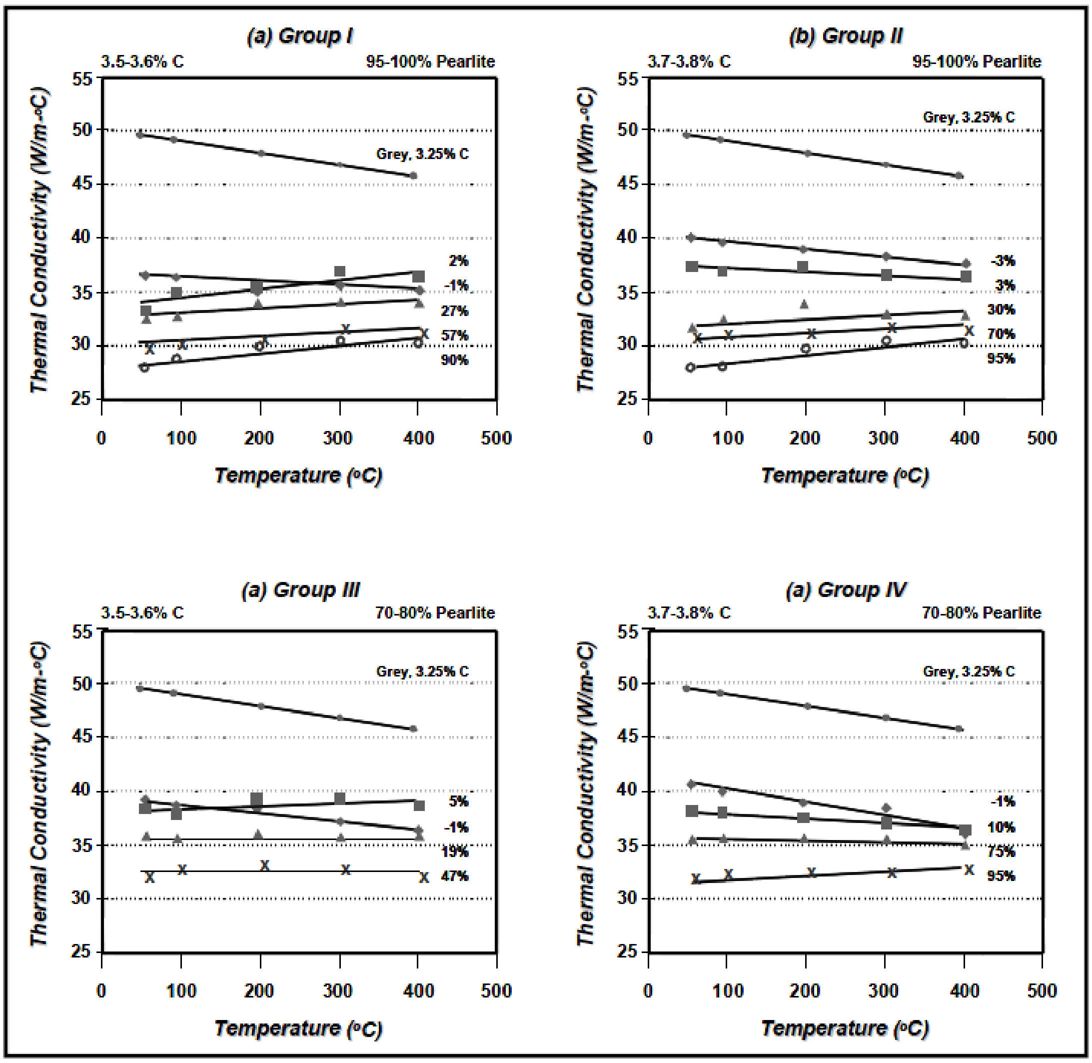

Figure 6.5 : Thermal conductivity of cast irons as a function of nodularity, carbon content and pearlite content. [2]

6.2. Material Model

In materials where the viscous properties within the plastic range play an important role it is necessary to apply the elasto-viscoplastic constitutive relations. We can cite the following elasto-viscoplastic models for example: Perzyna, Chaboche, Aubertin, Lehmann-Imatani , Miller, Bodner-Partom, Krempl, Tanimura, Krieg-Swearengen-Jones, Walker, Korhonen-Hannjula-Li, Freed-Virrilli.. Their relatively large number shows that they are not universal and can be applied only under certain conditions or for a limited range of materials, as shown in

Figure6.6 and Figure6.7 This constitutive model is suitable for analysis of isotropic materials (mainly metals at high temperatures) in the range of small inelastic strains.

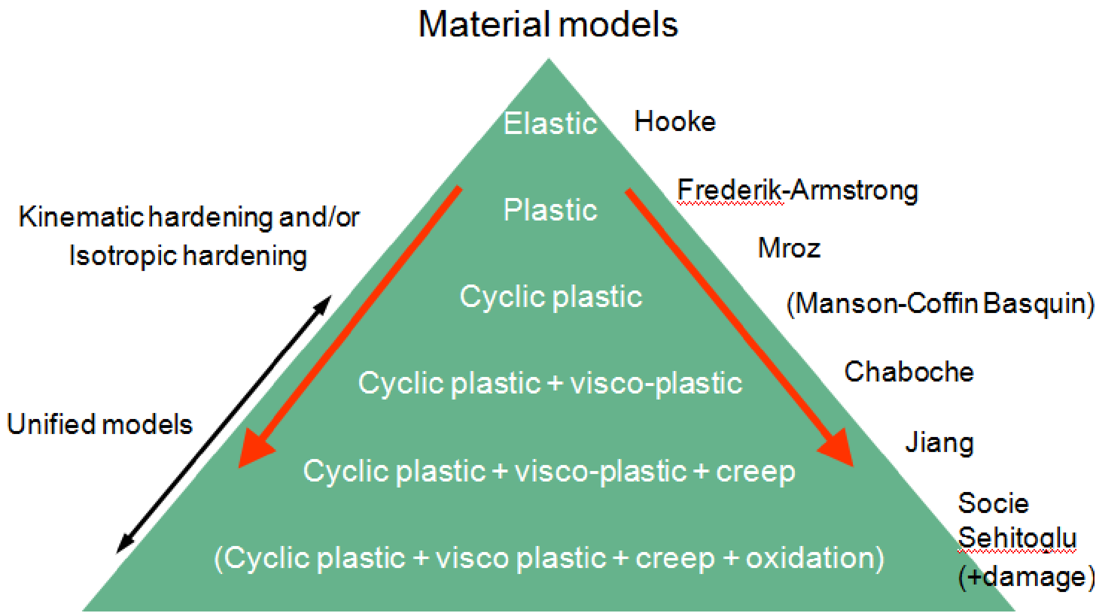

Figure 6.6 : Material models. [5]

Elasticity + plasticity + visoplasticity + oxidation *non linear*
Sehitoglu 1996

Elasticity + plasticity + viscoplasticity *non linear*
Modified Chaboche 1986, Jiang 1993

Elasticity + plasticity *linear or non linear*
- Linear kinematic hardening: Prager 1956
- Non linear kinematic hardening: Armstrong-Frederick 1966
- Isotropic hardening: Ramberg-Osgood 1943
- Combined: Chaboche 1979

Elasticity + ideal plasticity *bilinear*
Mohr-Coulomb 1900

Elasticity *linear*
Hooke 1678

Figure 6.7 : Material models history. [6]

6.3. The Chaboche Model

Proposed by Chaboche and his co-workers (1979, 1991), this model is based on a decomposition of non-linear kinematic hardening rule proposed by Armstrong and Frederick. This decomposition is mainly significant in better describing the three critical segments of a stable hysterisis curve. These three segments are:

1. The initial modulus when yielding starts,
2. The nonlinear transition of the hysterisis curve after yielding starts until the curve becomes linear again,
3. The linear segment of the curve in the range of higher strain.

To improve the ratcheting prediction in the hysterisis loop, Chaboche et al. (1979), initially proposed three decompositions of the kinematic hardening rule, corresponding to the above three segments of the hysterisis curve. Using this decomposition, the ratcheting prediction improved as compared to the A-F model. In the same work, Chaboche (1986) analyzed three models to describe kinematic hardening behavior. The first model that was studied uses independent multiyield surfaces as proposed by Mroz (1967). This model is useful in generalizing the linear kinematic hardening rule. It also enables the description of:

- Tthe nonlinearity of stress-strain loops, under cyclically stable conditions,
- The Bauschinger effect, and
- The cyclic hardening and softening of materials with asymptotic plastic shakedown.

The shortcoming of this model is its inability to describe ratcheting under asymmetric loading conditions.

The second type of models used only two surfaces, namely the yield and the bounding surfaces, to describe the material. The Dafalias-Popov (1976) model was chosen under this category, as it shows the following differences against the Mroz (1967) model:

- It uses two surfaces whereas Mroz (1967) uses a large number of surfaces
- In terms of the general transition rule for the yield surface, the Mroz formulation had an advantage over this model

- This model gives a function to describe a continuous variation of the plastic models, thus enabling description of a smooth elastic-plastic transition.

In the Mroz (1967) model, the number of variables needed for the description of ratcheting is very high and for cyclic stabilized conditions no ratcheting occurs. In the two-surface model, the updating procedure to describe a smooth elastic-plastic transition and simulate ratcheting effects leads to inconsistencies under complex loading conditions.

The nonlinear kinematic hardening rule is an intermediate approach of the models that uses differential equations that govern the kinematic variables. The varying hardening modulus can be derived directly based on these equations, whereas in the

case of the Mroz (1967) model, non-linearity of kinematic hardening was introduced by the field of hardening moduli associated with several concentric surfaces. In the case of the Dafalias and Popov (1976) model, it was done by continuously varying the hardening modulus, from which the translation rule of the yield surface is deduced.

It was later found that this model tends to greatly over-predict ratcheting in the

case of normal monotonic and reverse cyclic conditions. To overcome these pitfalls, Chaboche (1991) introduced a fourth decomposition of the kinematic hardening rule based on a threshold. This fourth rule simulates a constant linear hardening with in a threshold value and becomes nonlinear beyond this value. With the use of this fourth decomposition, the over-prediction of ratcheting is reduced and there is an improvement in the hysterisis curve. This is because, with in the threshold, the recall term is ignored and linear hardening occurs as it did without the fourth rule. Beyond the threshold the recall term makes the hardening non-linear again and reduces the ratcheting at a higher rate to avoid over-prediction.

6.3.1 Deformation modeling options

The constitutive equations give a relation between stresses and strains. Here rate constitutive equations are considered which are suitable for materials which show small elastic strains only, whereas the inelastic strain may be large. Therefore rate constitutive are typically used for metals. The Cauchy stresses σ are given in terms of the Jaumann rate

$$\overset{\circ}{\boldsymbol{\sigma}} = \mathbf{C}^e : \left(\dot{\boldsymbol{\varepsilon}} - \dot{\boldsymbol{\varepsilon}}^t - \dot{\boldsymbol{\varepsilon}}^{in}\right) + \frac{\partial \mathbf{C}^e}{\partial \theta} : \mathbf{C}^{e^{-1}} : \boldsymbol{\sigma}\dot{\theta}\,. \tag{6.1}$$

$\dot{\boldsymbol{\varepsilon}}$, $\dot{\boldsymbol{\varepsilon}}^{th}$ and $\dot{\boldsymbol{\varepsilon}}^{in}$ are the total, the thermal and the inelastic strain rates, θ is the temperature and Ce the isotropic elasticity tensor of the infinitesimal theory

$$\mathbf{C}^e = \frac{\mathrm{E}\nu}{(1+\nu)(1-2\nu)}\mathbf{1}\otimes\mathbf{1} + \frac{\mathrm{E}}{(1+\nu)}\mathbf{I} \tag{6.2}$$

with temperature dependent Young's modulus E and Poisson's ratio ν . The thermal strains are assumed to be small and isotropic:

$$\dot{\boldsymbol{\varepsilon}}^t = \alpha^{\mathrm{t}}_{\mathrm{dif}}\dot{T}\mathbf{1}\,. \tag{6.3}$$

The differential coefficient of thermal expansion $\alpha^{\mathrm{t}}_{\mathrm{dif}}$ has the meaning of the slope of the thermal strain-temperature curve and is related to the secant definition of the coefficient of thermal expansion $\alpha^{\mathrm{t}}_{\mathrm{sec}}$ through:

$$\alpha^{\mathrm{t}}_{\mathrm{dif}} = \frac{\partial \alpha^{\mathrm{t}}_{\mathrm{sec}}}{\partial \theta}\dot{\theta} + \alpha^{\mathrm{t}}_{\mathrm{sec}}\,. \tag{6.4}$$

A general form of the inelastic flow rule is given by

$$\dot{\boldsymbol{\varepsilon}}^{in} = \lambda\mathbf{n}\,. \tag{6.5}$$

Here, according to the associative inelasticity theory the flow direction n corresponds to the outward normal of a yield function φ in stress space, i.e. n = ∂φ / ∂σ . For φ ≤ 0 the set of stress states is defined where the material behaves elastically in the sense that ε& in = 0 . λ is a multiplier giving the amount of inelastic flow. For rate dependent, viscoplastic material behavior (vp) the stresses are not bounded and the viscoplastic multiplier λvp is given explicitly as function of the overstress φ > 0 . Here the overstress expression given in Chaboche (1989) is used:

$$\lambda^{\mathrm{vp}} = \left\langle \frac{\phi}{\mathrm{K}} \right\rangle^{\mathrm{n}} \tag{6.6}$$

where K and n are temperature dependent parameters characterizing the viscous material behavior. The rate dependent flow rule is used if iplstmd = 0 is set. In the rate independent plasticity theory, which is used by setting iplstmd = 1, the stresses are bounded to lie on the yield surface φ = 0 when inelastic flow occurs, so that the plastic multiplier λ p is determined implicitly through the loading/unloading conditions λ p ≥ 0 ,φ ≤ 0 and λ pφ = 0 . Beside the stresses σ , φ can be a function of additional tensorial and scalar variables describing irreversible internal rearrangements in the material. Here, attention is restricted to second order tensorial variables q and scalar variables q for which evolution equations with the following general structure are considered:

$$\overset{\circ}{\mathbf{q}} = \lambda \mathbf{n}^{\mathrm{q}}(\boldsymbol{\sigma}, \mathbf{q}, q) - \mathbf{m}^{\mathrm{q}}(\boldsymbol{\sigma}, \mathbf{q}, q)$$
$$\dot{q} = \lambda n^{q}(\boldsymbol{\sigma}, \mathbf{q}, q) - m^{q}(\boldsymbol{\sigma}, \mathbf{q}, q) \tag{6.7}$$

The first terms are dynamic contributions being active in case of inelastic loading, and the second terms are static contributions taking place also if elastic loading is present. This structure is governed by most classical kinematic hardening rules where q represents a backstress, Armstrong & Frederik (1966), Chaboche (1986,1989), Ohno & Wang (1993) and Jiang & Sehitoglu (1996). Scalar internal variables are within this framework e.g. isotropic hardening variables, Chaboche (1986,1989), and the porosity, Gurson (1977).

Von-Mises' yield function for plastically incompressible material behavior Most frequently used yield function in metal applications is the von-Mises yield function which specifies plastically incompressible material behavior. Mises materials are specified setting igurson = 0.

The Mises yield function considering isotropic and kinematic hardening reads:

$$\phi^{M} = \sqrt{\frac{2}{3}(\boldsymbol{\sigma}'-\boldsymbol{\alpha}'):(\boldsymbol{\sigma}'-\boldsymbol{\alpha}')} - \sigma_F . \tag{6.8}$$

The first term corresponds to the von-Mises equivalent stress. α is a backstress, inducing a kinematic hardening effect by a translation of the yield surface. F σ is the isotropic hardening variable, giving the current radius of the yield surface in the deviatoric plane. Assuming isotropic strain hardening, F σ can be modeled as combination of a nonlinear and a linear part, Simo & Hughes
(2000),

$$\sigma_F = \sigma_Y + Q_\infty(1 - \exp[-b\bar{\varepsilon}]) + h\bar{\varepsilon} . \tag{6.9}$$

σ , ∞ Q , b and h are the initial yield stress, the saturation stress of the nonlinear part, the transition constant of the nonlinear part and the hardening modulus of the linear part. The accumulated or equivalent inelastic strain ε follows from integration of the equivalent inelastic strain rate and therefore is an ever increasing variable.

6.3.2 Kinematic hardening law

To get a better accordance with experiments, Chaboche (1986,1989) introduced the backstress tensor α as sum of several parts:

$$\boldsymbol{\alpha} = \sum_{iaa=1}^{\text{naa}} \boldsymbol{\alpha}^{iaa} .$$

(6.10)

The number of backstresses to be used naa is specified in the input card. For every part αiaa an evolution equation is specified. Here equations also found in Chaboche (1986,1989) are used, namely

$$\overset{o}{\boldsymbol{\alpha}}{}^{iaa} = \frac{2}{3} \mathrm{C}^{iaa} \dot{\boldsymbol{\varepsilon}}^{vp} - \gamma^{iaa} \hat{\varphi}^{iaa} \boldsymbol{\alpha}^{iaa} \dot{p} - \mathrm{R}^{iaa} \boldsymbol{\alpha}^{iaa} + \frac{\partial C^{iaa}}{\partial \theta} \frac{1}{C^{iaa}} \boldsymbol{\alpha}^{iaa} \dot{\theta} .$$

(6.11)

The first term corresponds to the linear Prager-Ziegler hardening law and the second term a recovery term, resembling to the classical Armstrong & Frederik (1966) nonlinear kinematic hardening law (except the function ϕˆiaa specified later). Both are dynamic, i.e. taking place only when the material yields. The third term is a static recovery term, i.e. recovery with time. The fourth term contributes to hardening evolution in case of non-isothermal loading and is discussed in Chaboche (1993). However, experience showed that for some material parameters this term yields a worse convergence in the finite-element program due to softening, which can be bypassed by switching this term off, i.e. setting imtdpnt = 0 .

Ciaa is the hardening modulus, γiaa the transition constant and Ciaa / γiaa is the saturation stress of the kinematic hardening variable in one-dimensional problems. Riaa is the static recovery parameter. All these parameters are functions of temperature. Actually Ciaa / γiaa is used in the implementation, i.e.

$$\overset{o}{\boldsymbol{\alpha}}^{iaa} = \gamma^{iaa}\left(\frac{2}{3}\frac{C^{iaa}}{\gamma^{iaa}}\dot{\varepsilon}^{vp} - \hat{\varphi}^{iaa}\boldsymbol{\alpha}^{iaa}\dot{p}\right) + \frac{2}{3}H^{iaa}\dot{\varepsilon}^{vp} - R^{iaa}\boldsymbol{\alpha}^{iaa}$$
$$+\frac{\partial\left(C^{iaa}+H^{iaa}\right)}{\partial\theta}\frac{1}{\left(C^{iaa}+H^{iaa}\right)}\boldsymbol{\alpha}^{iaa}\dot{\theta}$$

(6.12)

To specify only linear kinematic hardening (γiaa = 0), the separate hardening modulus Hiaa is introduced. φ_{∞}^{iaa} is taken to be, Chaboche (1989),

$$\hat{\varphi}^{iaa} = \varphi_{\infty}^{iaa} + (1-\varphi_{\infty}^{iaa})\exp(-\omega^{iaa}X).$$

(6.13)

Here X acts as a replacement character for different arguments. For $X=\sqrt{3/2\varepsilon^{in}}$ tertiary creep can be modeled, for X = ε cyclic hardening and softening. The parameter φ_{∞}^{iaa} is a saturation value and ω^{iaa} a transition constant, both temperature dependent. If iaatyp = 0 , X = ε is used for all backstresses. If iaatyp = 1, $X=\sqrt{3/2\varepsilon^{in}}$ is used for the first backstress (i.e. iaa = 1) and X = ε for all others (i.e. iaa > 1).

Non-Unified inelastic strain rate

A non-unified inelastic strain rate is

$$\dot{\varepsilon}^{in} = \sum_{iee=1}^{nee}\lambda^{iee}\mathbf{n}^{iee}$$

(6.14)

where nee is the number of inelastic strain rates used and is specified in the input deck.

The decomposition of the inelastic strain rate in nee parts can be distinctly motivated in view of high temperature applications since the deformation mechanisms acting are depending on the loading, as can be seen form deformation maps, see e.g. Riedel (1987): Diffusion processes are dominating the macroscopic deformation when low stresses and high temperatures are acting, whereas dislocation glide dominates for high stresses at moderate temperatures. In this spirit von Hartrott et. al (2005) use nee = 2 inelastic strain rates, one for diffusion based the other for dislocation based deformations. A similar decomposition can be found in Schemmel (2003) and Klenk et. Al (2005). The decomposition of the viscoplastic rate of deformation into a transient and a stationary part is pursued by Kobayashi et. al (2003). This non-unified framework is questionable, when porosities are present. The failure of the material as well as stress induced void nucleation can not be reasonable incorporated if nee > 1.

6.3.3 Implementation and solution options

The implementation of the von Mises materials allows for calculations with three dimensional continuums elements, with axisymmetric and plane strain elements as well as plane stress and shell elements. The Gurson materials, however, can not be used with plane stress and shell elements. The rate constitutive equations introduced before require incremental objective algorithms. In commercial finite-element software such algorithms are typically implemented so that the actual time integration of the constitutive equations can be performed with standard small strain stress update algorithms. If implementations are available like in ABAQUS or ANSYS or only small strains and small rotations are to be considered (i.e. a linear geometry) on sets ilrgdf = 0 . If not ilrgdf = 1 specifies the use of an incremental objective algorithm due to Weber et. al (1990) and ilrgdf = 2 the Hughes & Winget algorithm (1980) in terms of the implementation described in Simo & Hughes (2000). Both algorithms are based on a rotated configuration, see Simo & Hughes (2000).

An implicit integration of the ordinary differential equations is

$$\mathbf{G} = -\mathbf{Y}_{n+1} + \mathbf{Y}_{n} + \Delta t\dot{\mathbf{Y}}_{n+1} = \mathbf{0} \tag{6.15}$$

where Δt = tn − tn+1 is the time increment, Y n+1 the unknowns to be omputed (i.e. the stresses and internal variables), Yn are the known values of the last time step and Y n + 1 & are the rates at t n+1 . In case of rate independent material behavior the incremental consistency condition ϕ_{n+1} = n+ φ has to be added to the residual equation (3.29). In case of an elastic load step, equation (3.29) can be solved in closed form. In case of inelastic loading a closed form solution can in general not be obtained. A Newton scheme is then applied according to

$$\mathbf{Y}_{n+1}^{(i+1)} = \mathbf{Y}_{n+1}^{(i)} - \alpha^{(i)}\left[\mathbf{A}^{(i)}\right]^{-1}\mathbf{G}^{(i)} \tag{6.16}$$

α (i) is a line search parameter, intended to obtain a globally convergent Newton scheme. The line search algorithm can be activated by setting ilnsrng = 1. In general, activation of the line search algorithm increases stability and convergence rate and is therefore recommended. The Jacobian matrix

$$\mathbf{A}^{(i)} = \frac{\partial \mathbf{G}}{\partial \mathbf{Y}_{n+1}} \Big|_{\mathbf{Y}_{n+1}=\mathbf{Y}_{n+1}^{(i)}} \qquad \textbf{(6.17)}$$

Is computed analyitcally in the material routine. However it is possible to used a numerically computed Jacobian by setting inumjac = 1 or check the analytical one by setting inumjac = 2 . In this case, output of numerical and analytical Jacobian is plotted if an output is specified by setting the iwrite parameter. If an accuracy monitored integration is to be perfomed in a simulation, a step time control can be activated by setting TOLVP ≠ 0 . The positive value TOLVP ≠ 0 then corresponds to the maximal error allowed in the inelastic equivalent strain. Is the tolerance not achieved, the finite-element program is forced to repeat the increment with smaller time increment Δt . The Newton iteration equation (3.29) is considered converged if the the residual norm is small enough in the sense that the normalized residual norm is less than = 10−4 G Tol . If no convergence is achieved within 20 iterations, the Newton scheme is terminated. Divergence can occur e.g. if the time increment is to large or due to instabilities finite-element program proposes unrealistically large strain increments. In these cases the finite-element program is forced to repeat the increment with smaller time increment Δt . If output is activated by specifying iwrite , a message is displayed at the output element and integration point starting with ***. If iwrite = 2 is set, at each integration point that requires a time increment reduction a message is written starting with +++. The parameter PNEWDT in these messages refers to the factor of reduction of the time increment:

$\Delta t_{neu} = \mathrm{PNEWDT} \cdot \Delta t_{alt}$.

If locally in certain regions of the domain large strains occur so that no convergence could be achieved at an integration point but the remaining parts are loaded almost elastically, it is reasonable to subdivide a time increment into several substeps within the material routine. With this substepping technique the computation time can be reduced. By setting the parameter MAXSUB > 1 sub stepping is active, where MAXSUB > 1 specifies the maximal number of sub steps allowed. In general, MAXSUB = 8 is a good choice. The sub stepping technique can also be used in an accuracy controlled simulation, often yielding a significant reduction of the computation time. The consistent tangent moduli ∂σ ∂Δε + / n 1 are required for a quadratically convergent solution of the equilibrium equations. The moduli are compute analytically within the material routine. By setting inumtan = 1 a numerical computation can be demanded and for inumtan = 2 the numerical and analytical moduli are compared and printed to the output if the iwrite parameter is set. The consistent tangent moduli do not influence the result but the convergence behavior of the equilibrium iterations.

If Gurson's model is used with stress-induced void nucleation, the consistent tangent is unsymmetric. It should then be checked, if the use of the unsymmetric solver in the finite-element program is necessary, since it can increase the computation time up to a factor of four. By setting istbck = 1, the eigenvalues of the consistent tangent are computed. The eigenvalue information is then important, if softening in the material occurs and an implicit finite-element solver gets stability problems resulting in very small time increments. Softening is present when the consistent tangent has negative eigenvalues. However, a negative eigenvalue is not a sufficient condition for instability. A message is displayed if output is active.

6.3.4 Deformation parameter

The material parameters introduced in the preceding section can be summarized as follows:

- Thermo-elasticity: E [MPa], ν [-], $\alpha^{\mathrm{t}}_{\mathrm{dif}}$ [1/°C]
- Inelasticity (for each of the $iee = 1,\ldots,\mathrm{nee}$ strain rates)
  - Damage:
    q_1^{iee} [-], q_2^{iee} [-], q_3^{iee} [-], f_0^{iee} [-], f_C^{iee} [-], f_F^{iee} [-],
    $\mathrm{f}_N^{\varepsilon\,iee}$ [-], $\mathrm{s}_N^{\varepsilon\,iee}$ [-], ε_N^{iee} [-], $\mathrm{f}_N^{\sigma\,iee}$ [MPa], $\mathrm{s}_N^{\sigma\,iee}$ [MPa], σ_N^{iee} [MPa]
  - Viscosity:
    K^{iee} [MPa], n^{iee} [-]
  - Isotropic hardening:
    σ_Y^{iee} [MPa], Q_∞^{iee} [MPa], b^{iee} [-], h^{iee} [MPa]
  - Kinematic hardening (for each of the $iaa = 1,\ldots,\mathrm{naa}$ backstresses):
    $\mathrm{C}^{iee,iaa}$ [MPa], $\gamma^{iee,iaa}$ [-], $\mathrm{H}^{iee,iaa}$ [MPa], $\varphi_\infty^{iee,iaa}$ [-], $\omega^{iee,iaa}$ [-], $\mathrm{R}^{iee,iaa}$ [1/s].

The use of gradient based optimization methods for parameter identification requires the sensitivities of the stresses with respect to the material parameters. The computation of the sensitivities is activated setting imatpid = 1. Numerical derivatives of the residuum with respect to the parameters are computed via inumres = 1. The analytical and numerical derivatives can be compared with inumres = 2 provided that output is active using iwrite . Deformation solution dependent state variables The stresses and strains are not stored in the solution dependent state variables (SDV) but made available in general by the finite-element program used. The variables stored in the SDV's are

- thermal strains $\boldsymbol{\varepsilon}^{t}$
- inelastic strains $\boldsymbol{\varepsilon}^{in}$
- backstresses $\boldsymbol{\alpha}^{ivp,iaa}$
- inelastic equivalent strains $\bar{\varepsilon}^{ivp}$
- inelastic equivalent strains of matrix material $\bar{\varepsilon}_{M}{}^{ivp}$
- porosity f^{ivp}, porosity due to growth $f_{gr}{}^{ivp}$, strain and stress controlled nucleation $f_{nucl}^{\varepsilon}{}^{ivp}$ and $f_{nucl}^{\sigma}{}^{ivp}$ and effective porosity f^{*ivp}
- flag for elements that failed ($ifailed = 1$)
- maximal nucleation stress $\lfloor \sigma_{C}{}^{ivp} \rfloor_{\max}$
- maximal nucleation strain $\lfloor \varepsilon_{C}{}^{ivp} \rfloor_{\max}$
- flag for inelastic yielding ($ivpflag = 1$)

6.3.5 Lifetime prediction options - classical DTMF

The implemented lifetime model uses the damage parameter D_{TMF} , Schmitt et. al (2002). This damage parameter is a generalization of the damage parameters Z_D due to Heitmann (1983) and D_{CF} due to Riedel (1987) which are intended for materials exhibiting Masing-behaviour. D_{TMF} can be applied to nonisothermal load cycles with arbitrary form of the hysteresis and is given by

$$D_{TMF} = Z_D F \text{ where}$$

$$Z_D = Z_D^e + Z_D^{in} \text{ and } Z_D^e = 1{,}45 \frac{\Delta\sigma_{I,eff}^2}{\sigma_{cy} E}, \; Z_D^{in} = \frac{2{,}4}{\sqrt{1+3N}} \frac{\Delta\sigma_I^2}{\sigma_{cy}\Delta\sigma_e} \Delta\varepsilon_e^{in} \tag{6.18}$$

Z and in

ZD are the elastic and inelastic portion of the damage parameter ZD.

The quantities appearing in D_{TMF} are illustrated in Figure 6.8

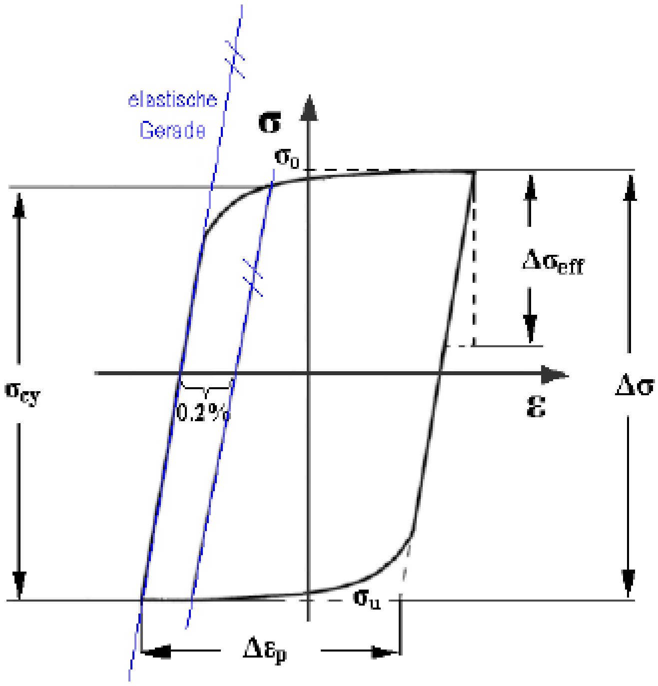

Figure 6.8 : Characteristics of the hysteresis loop needed for the damage parameter TMF. [9]

σ_{cy} is the cyclic yield stress, N the Ramberg-Osgood hardening exponent of the cyclic stress-strain curve and E is Young's modulus. The SCHWINGBREITEN of the equivalent stress, the maximal principal stress and the inelastic equivalent strain

$$\Delta\sigma_e = \sqrt{\frac{2}{3}\left(\boldsymbol{\sigma}' - \boldsymbol{\sigma}'^0\right) : \left(\boldsymbol{\sigma}' - \boldsymbol{\sigma}'^0\right)}$$

$$\Delta\sigma_I = \left|\sigma_H - \sigma_H^0\right|$$

$$\Delta\varepsilon_e^{in} = \sqrt{\frac{2}{3}\left(\boldsymbol{\varepsilon}^{in\,\prime} - \boldsymbol{\varepsilon}^{in\,\prime 0}\right) : \left(\boldsymbol{\varepsilon}^{in\,\prime} - \boldsymbol{\varepsilon}^{in\,\prime 0}\right)} \tag{6.19}$$

The upper index 0 refers to the starting point of a hysteresis branch and $\sigma_H = \max\left(\left|\sigma_I\right|, \left|\sigma_{III}\right|\right)$ is according to amount the largest principal stress. The effective SCHWINGBREITE in equation (3.1) accounts for crack closure and is defined as

$$\Delta\sigma_{I,eff} = \frac{3.72}{(3-R)^{1.74}}\Delta\sigma_I \tag{6.20}$$

R is the ratio of lower stress to upper stress.

The function F in equation (4.1) includes the lifetime shortening effect of holding times and higher temperature in the model. The number of cycles to fracture is computed form the power law relation

$$N_f = \mathrm{A}\,(D_{TMF})^{-\mathrm{B}}. \tag{6.21}$$

A and B are adjustable parameter, where from fracture mechanics B should be in the order of one.

6.3.6 Implementation and evaluation options

To evaluate the lifetime of a component with finite-elements a typical load cycle has to be taken and the resulting stress strain hysteresis is to be evaluated. This requires the input of hysteresis branches which have to be defined by the time they begin and the time they end. Several branches can be considered where the damage parameters are then computed as mean average of the damage parameters of each hysteresis branch. The number of branches (half cycles) to be used is set by nhfcy . The associate begin and end times are input in t_lftbihfcy and t_lfteihfcy for ihfcy = 1,...,nhfcy . Since the stress-strain hysteresis are not necessarily closed, at least the loading and the unloading branch should be considered, i.e. nhfcy = 2 . Additionally a time has to be specified when all branches have been calculated and the lifetime is to be evaluated according to equations (4.7) or (4.8). This time is specified in t_nf .

For nonisothermal loading the parameters E , σ_{cy} and N are taken as the mean average of the minimal and the maximal value occurring in one hysteresis branch if one sets iltdpnt = 1. If one sets iltdpnt = 0 the current values are taken.

- Lifetime parameter

The lifetime parameters introduced in the preceding section can be summarized as follows:

- Constant parameters:

α , Q/R , T0 , γ L , T L , s L , A(1) , B(1) , A(2) , B(2) , σ f

- Temperature dependent parameters:

σ_{cy} , N , m, σ_y , ε_f

No implementation is done yet to compute analytical sensitivities of the lifetime with respect to the parameters. Lifetime solution dependent state variables

The solution dependent state variables of the lifetime models are

- Flag for storing the starting values of the hysteresis half cycle (first increment of hysteresis) ($ifirst_{ihfcy} = 1$)
- Stresses of starting point $\boldsymbol{\sigma}^0{}_{ihfcy}$
- Inelastic strains of starting point $\boldsymbol{\varepsilon}^{in\,0}{}_{ihfcy}$
- Largest principal stress according to amount $\sigma_{H\,ihfcy}$
- Principal direction $\mathbf{n}_{H\,ihfcy}$ corresponding to $\sigma_{H\,ihfcy}$
- Current crack length at fracture $a_{f\,ihfcy}$
- Maximal and minimal values of σ_{cy} , N , E and ε_f in half cycle
- $Z^e_{D\,ihfcy}$: elastic part of $Z_{D\,ihfcy}$ (first term)
- $Z^{in}_{D\,ihfcy}$: inelastic part of $Z_{D\,ihfcy}$ (second term)
- Total $Z_{D\,ihfcy}$
- Flag if fracture occurs in the cycle ($ifrac_{ihfcy} = 1$)
- Integral expression $F^{\mathrm{int}}{}_{ihfcy}$ in correction function F_{ihfcy}
- correction function F_{ihfcy}
- damage parameter $D_{TMF\,ihfcy}$
- averaged damage parameter of half cycles D_{TMF}
- lifetimes $N_f^{(1)}$ and $N_f^{(2)}$ computed from averaging damage parameter of half cycles and total lifetime N_f

7. MATERIAL TESTS

It is aim to predict deformation and lifetime heads made of vermicular cast iron, which has the nominal composition of CGI450, under thermomechanical loading. To this end, the compupapional methods developed at the Fraunhofer Institute for Mechanics of Materials IWM should be applied. The methodology comprises models for cyclic plasticity and microcrack growth, a finite element implementation and a test procedure determine the model parameters.

For the cast iron CGI450 models were devoloped, however the mechanical properties depend on the casting process and the chemical composition. Thus, the vermicular cast iron should be investigated with a reduced test program at first. Then, an appropriate scaling aof model parameters for CGI450 can be attempted to describe deformation and lifetime of cast iron.

At three-part procedure is proposed, in part1, sample tests are done in the temperature range of interest in order to generate a data base for the comparision of cast iron and GJV450. If the material behaviour differs, additional tests are done to validate and to extend the data base in part 2. In part 3, the models edjusted to the cast iron by an appropriate scaling of models for CGI450.

7.1. Cyclic Plasticity Models

Time and temperature dependent cyclic plasticity models has been adjusted to large number of different high temperature materials (e.g. austenetic and ferritic steels and cast materials, nickel base alloys). The adjusted models are applied in motor and exhaust systems production as well as in power engineering. The models describe the deformation of the materials for different loading conditions, in particular for thermo-mechanical cyclic loadinngs. Cast iron exhibits due to the graphite particles an asymmetric behaviour in tension and compression. For this reason, the capabilities of the chaboche model and gurson model were combined. Thus, the time and temperature dependent cyclic plasticity as well as the effect of the porpsity caused by the graphite particles can be described.

To determine the model parameters, complex low-cycle fatigue (CLCF) tests are carried out. These CLCF tests consist of an unperiodic and periodic part. In the unperiodic part, different stain rates between e-3 1/s and e-5 1/s as well as hold times are used. A typical strain-time history of the unperiodic part of a CLCF test is shown in Figure 7.1 the loading history allows to measure effects of the loading rate as well as relaxation and cyclic hardening at a certain temperature in one single test. Thus, the number of necessary test can be reduced significantly. In the periodic part of CLCF tests the specimens are cyled to failure at constant strain rate (e-3 1/s) and constant amplitude. Hold times can be introduced at maximumor minimum strain in the periodic part of the test is also reproduced well.

Figure 7.3 shows the model periodic of thermo-mechanical fatigue (TMF) tests. The symbols indicate the experimental data. The model prediction is indicated by the solid lines. The model parameters were detrmined from isothermal.

7.1.1. Microcrack growth and life time

Under LCF and TMF conditions microcracks are usually observed to nucleate during the first few percent of the lifetime in metallic materials. This means that the lifetime is determined by the growth of these microcracks to an unacceptable size or fracture. At the Fraunhofer IWM, life time models are developed and applied, which are passed on microcaracks and was applied to different high temperature components.
Figure 7.4 shows the damage parameter DTMF plotted over the measured number of cycles to failure Nf for iso-thermal LCF tests as well as TMF tests for CGI450. The fatigue life correlates very well with the damage parameter.

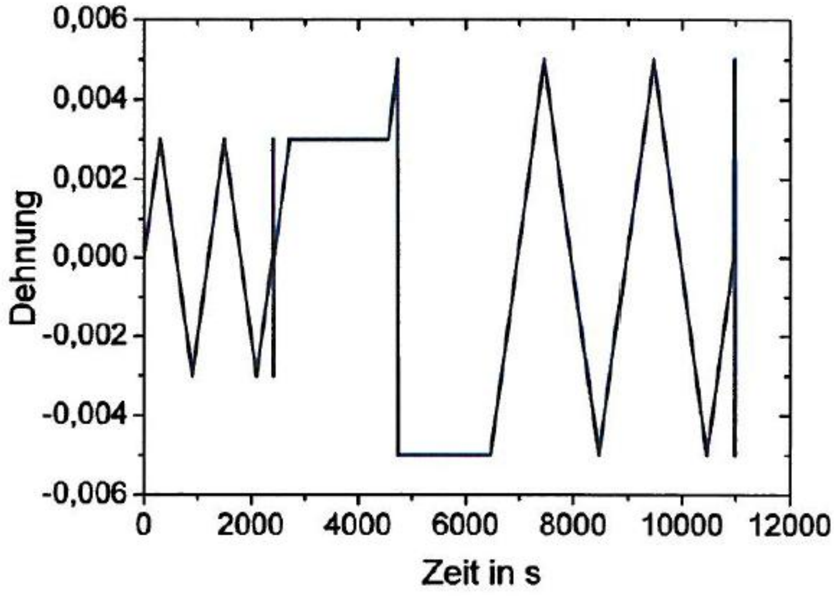

Figure 7.1 : Exemplary strein-time history applied to the speciemens. [12]

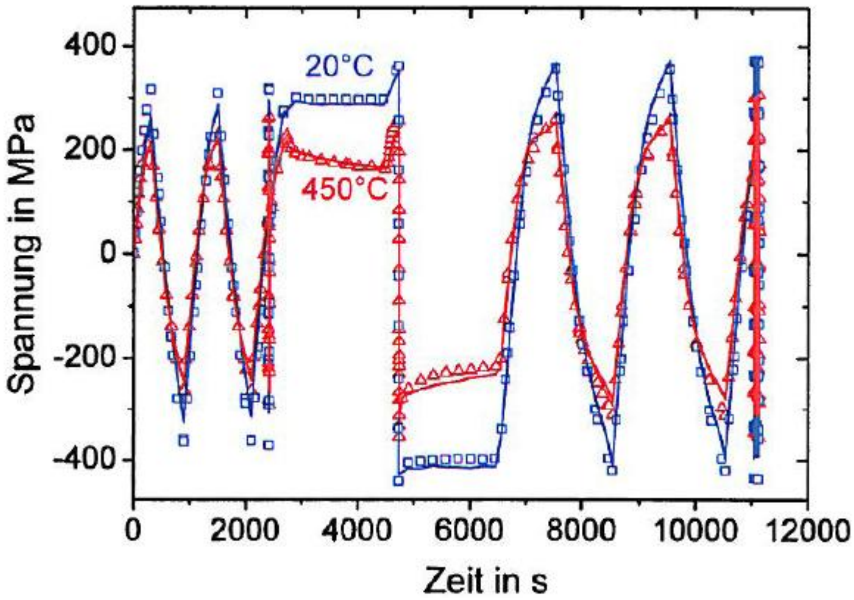

Figure 7.2 : Stress responses at different temperatures of the cast iron CGI450, symbols: experiment, line model prediction. [12]

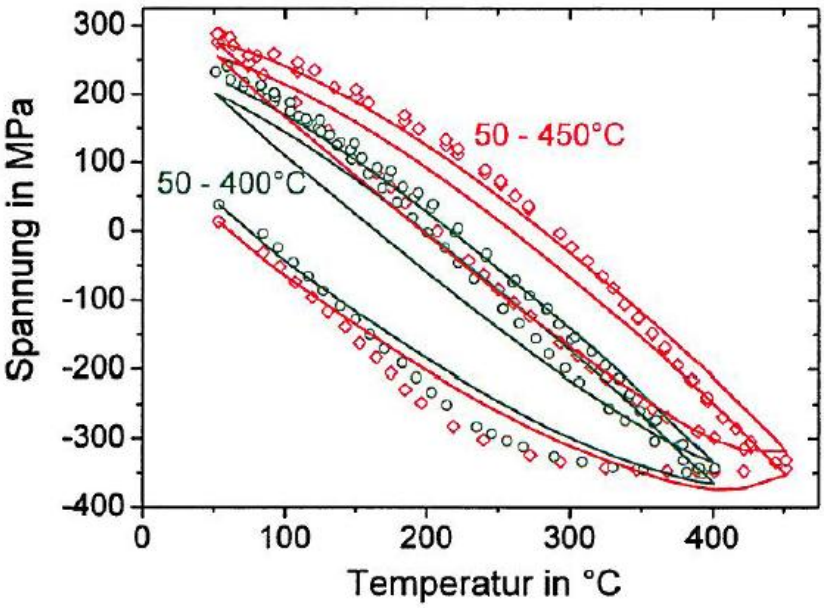

Figure 7.3 : Prediction of TMF Tests with the cast iron CGI450 symbols: experiment, line: model prediction. [12]

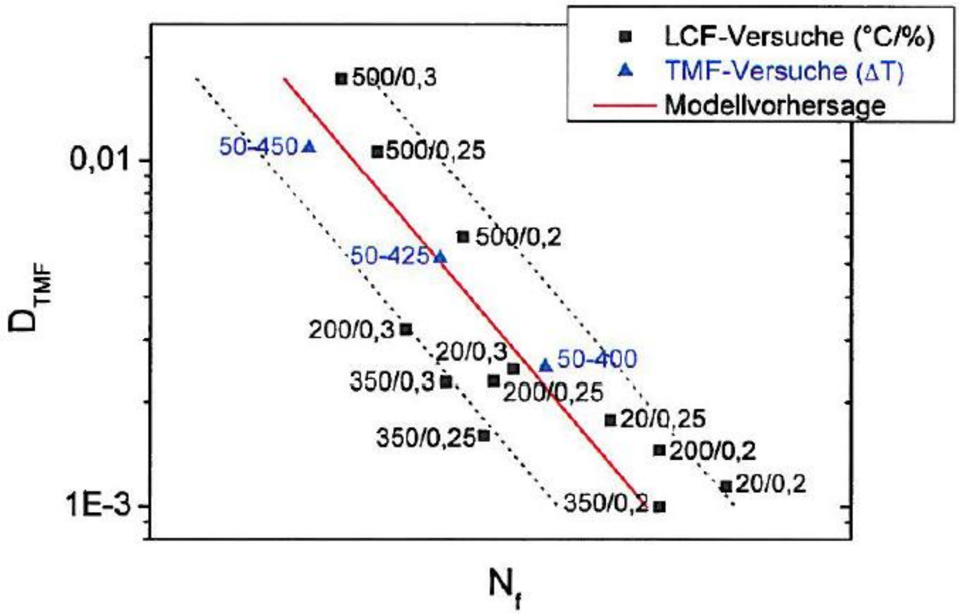

Figure 7.4 : LCF and TMF life prediction of the cast iron CGI450, the dotted line indicates the scatter band with factor two. [12]

Finite Element Implementation and Application to Components

The models for cyclic plasticity and fatigue life prediction were implemented at the Fraunhofer IWM in the Software ThoMat and are currently available for the finite element program ABAQUS/Standart. Within the software routine, the damage parameter DTMF evaluated and the number of cycles to failure is calculated for each location of the component.

Semi-finished parts are provided for the experimental characterization of the material. The semi-finished parts are processed at the workshop of Fraunhofer IWM. The geometry of the specimens is shown in Figure 7.5. The uniaxial tests are carried out in air atmosphere.

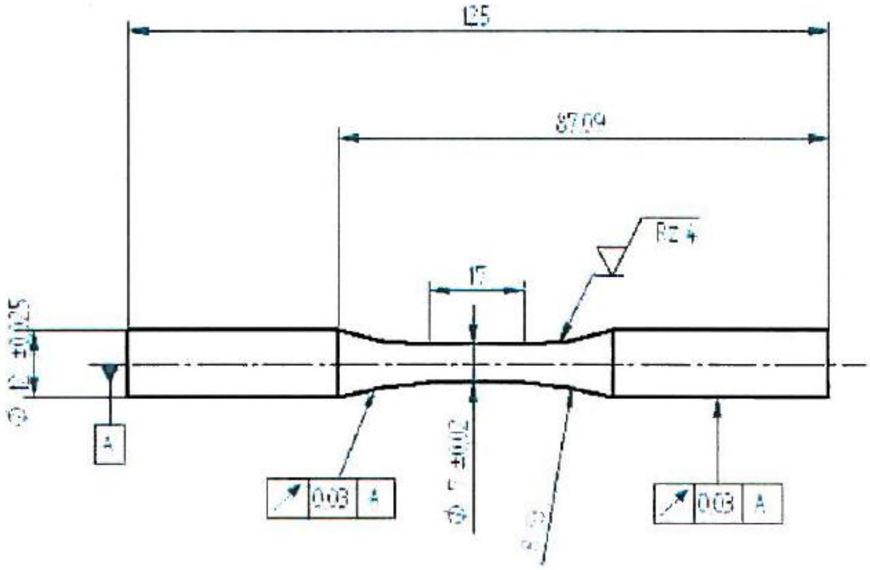

Figure 7.5 : Geometry of the specimens. [12]

7.1.2. Receiving inseption

The mechanical properties of cast materials depend on the solidification conditions. Therefore, it is recommended to compare the microstructure of the specimens with the microstructure at critical locations of the compnent. Furthermore, the semi-finishedparts should be investigated with respect to shrinkage cavities and voids.

- Grinding, etching, light microscopy, hardness profile
- Chemical composition
- Coefficient of thermal expansion (dilatometry)

7.1.3. Uniaxial tests

Manufacturing of The Specimens

Round tensile-compression specimens are manufactured according to Figure 7.5

Basic Set-Up

The basic set-up comprises the alignment of the testing machine, the calibration of the extensometer, the adjustment of the heating equipment (induction coils and furnace) the Labview configuration for the testing program, preliminary tests and further detail works at the testing machine.

7.1.4 Tensile tests and compression tests

At the temperatures, at which CLCF tests are carried out, a tensile test a compression test is carried out. The results are used to model the material behaviour at larger strains. Strain to fracture, yield strength and ultimate strength are determined by using specimens, as shown in Figure7.6

Figure 7.6 : Specimens of CGI450 material from cylinder head.

7.1.5 Incremental step tests

Isothermal strain controlled incremental step tests (Figure 7.7) are carried out. Cyclic stress-strain curves are extracted for small and larger strain amplitudes. For cast materials, the strain amplitude is identified at which the graphite inclusions have an affect on the stress-strain curve (tension-compression asymmetry)

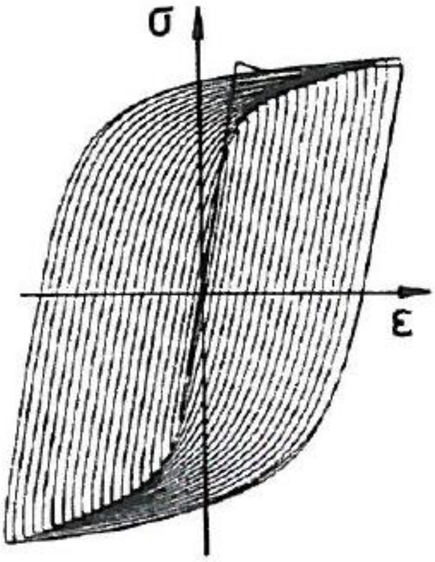

Figure 7.7 : Cyclic stress-strain curves obtained in incremental step tests.

7.2. CLCF Tests

Isothermal CLCF tests are carried out in the temperature range between room temperature and maximum 1050 C. The temperature levels are defined with the agreement of the cumtomer. The CLCF tests consist of an unperiodic and a periodic part. The amplitudes are chosen in agreement with the customer such that a maximum number of 5000 cycles to failure are obtained. The LCF tests are evaluated (stress-strain behaviour, correlation of measured fatigue lives with conventional damage parameters as Manson-Coffin, Smith-Watson-Topper, Ostergen)

7.2.1. TMF Tests

TMF Tests are carried out with service like loadings (temperature-time history). The loadings are chose in agreement with the customer such that a maximum number of 1000 cycles to failure are obtained.

7.2.2 Analysis of fracture surfaces

The fatigue lives of the specimens can be affected by voids and shrinkage cavities. The fracture surfaces and microstructure are investigated by means of ligth and electronic microscopy.

7.2.3 Scaling of the models parameters of the deformation model

The model parameters of the Chaboche modeli which were adjusted CGI450, are scaled, so that a best possible description of the experimantal data of tensile, compression, LCF and TMF for the cast iron.

7.2.4 Scaling of the model parameters of the lifetime model

The model parameters of the DTMF fatigue life model, which were adjusted CGI450, are scaled, so that a best description of the LCF and TMF tests of the cast iron.

An advantage of the faracture mechanics based damage parameter is the possibility to include the knowledge of the analysis of fracture surfaces.

8. FINITE ELEMENT MODEL RESULTS

In this study, the thermal-mechanical fatigue analysis of cylinder head is performed. The aim of the study is to determine the most critical region of cylinder head in terms of fatigue life.

Firstly, heat transfer analysis is performed and the temperature distribution of cylinder head is obtained. Then these results lead to structural analysis and at the end of the structural analysis, fatigue life distribution is achieved.

In this way, cylinder head produced from CGI 450 material is analysed faster and more economically without the need to collect engine and engine tests. In addition to cost advantages, pollution created by combustion of thousands liters of fuels is reduced by using gaseous fuels such as natural gas because diesel/gasoline is not used as fuel, thus an environmentally friendly CAE method is developed.

In addition to that, using sub-modeling allowed to focus the critical region. This technique provided that an easy modeling enhancement of these critical areas without having to resort to re meshing and reanalyzing the entire model. Reducing analysis costs is achieved by using this technique while providing detailed results in local regions of interest.

8.1. Temperature Distribution

After completion of 1D and 3D CFD analyses, gas / water temperature and HTC are obtained. This CFD analysis is a type of conjugate analysis, therefore metal temperature distirbution achieved at the same time.

Maximum temperature value is observed on the flame deck. The maximum temperature around 390 °C, as shown in Figure8.1 and Figure8.2

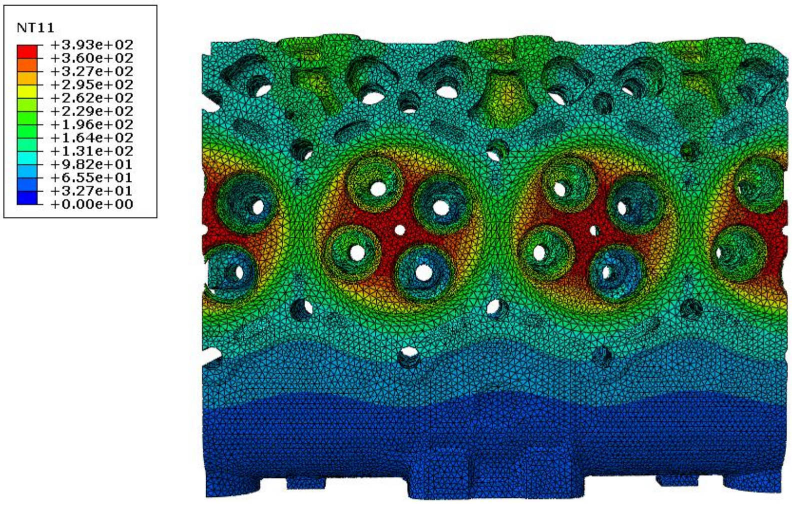

Figure 8.1: Temperature distribution for all model.

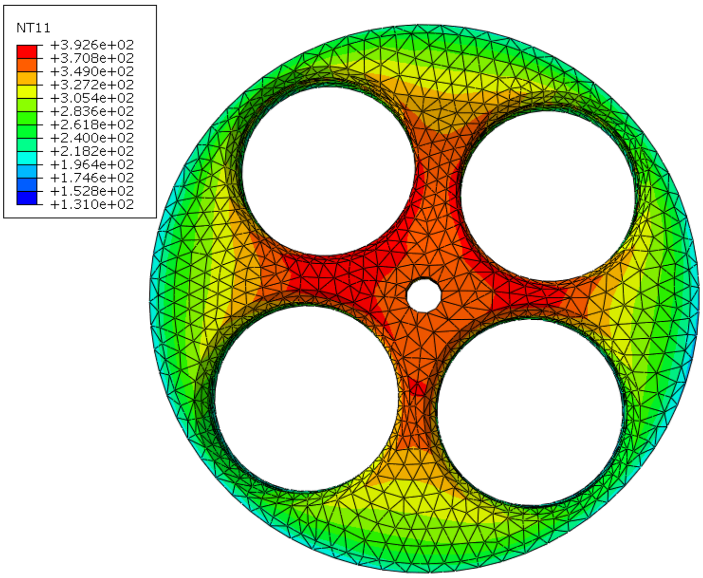

Figure 8.2 : Temperature distribution for Sub-model.

8.2. TMF Life Distribution

Cylinder head temperatures are acquired with the completion of thermal analysis. These thermal data and mechanical loads are used as input for structural analysis fatigue life cycle is found as a results of this analysis.

Minimum fatigue life cycle is acquired at the exhaust-exhaust valve bridge with 3500cycle, as shown in Figure8.3. This result shows that estimated critical region are incompliance with a heavy duty in terms of fatigue life criteria. Expected fatigue life is around 4000cyle for automotive applications. The life value is based on the previos thermomechanical dyno test.

So the structural analysis result prove out the cylinder head design and material selection for the Euro5 engine emission and 165bar peak fire pressure performance criteria.

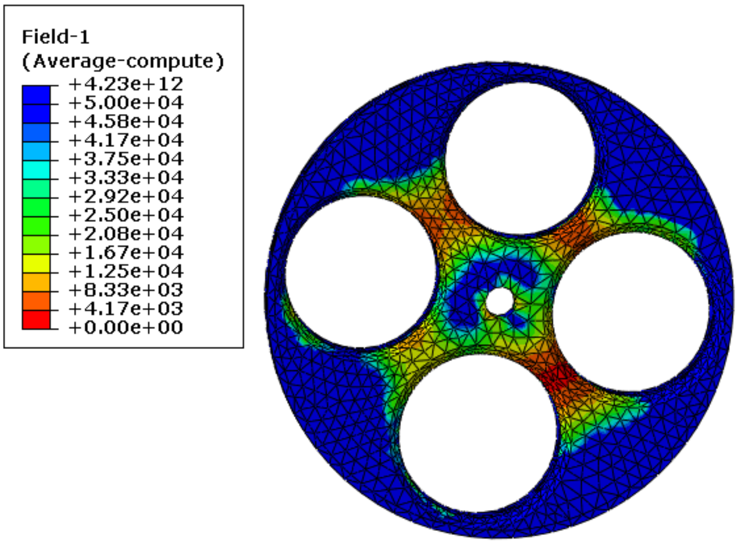

Figure 8.3 : TMF life distribution for Sub-model.

Table 8.1: TMF Life distribution for different nodes on sub-model.

Node ID	N of C to FTG
2673830	5.34E+03
2699228	3.84E+03
2673828	3.58E+03
2673888	4.50E+03
2699297	6.15E+03
2699274	5.52E+03
2699032	3.75E+03
2699043	3.38E+03
2699154	4.21E+03
2699212	4.30E+03
2699774	4.61E+03
2699772	4.76E+03
2699736	3.96E+03
2699737	3.29E+03
2699746	3.49E+03
2699726	4.64E+03
2699726	4.64E+03
2699787	4.55E+03
2704183	5.38E+03
2699746	3.49E+03
2699781	3.45E+03
2673887	3.76E+03
2703992	4.04E+03
2699227	4.36E+03

2699029	5.58E+03
2699027	4.45E+03
2699152	3.75E+03

REFERENCES

[1]**Ford Otosan,** 2012: Cylinder head finite element mesh procedure

[2]**Dawson, Dr. Steve** 1999 Compacted Graphite Iron:Mechanical and Physical Properties for Engine Design

[3] **W. Guesser, T. Schroeder , S. Dawson,** 2001: Production Experience With Compacted Graphite Iron Automotive Components, AFS 2001 release.

[4] **Luiz Guesser, Wilson,** 2003: Compacted Graphite Iron – a new material for diesel engine cylinder blocks, Brazilian MRS Meeting 2003

[5] **Y. P. Gong, C. J. Hyde1, W. Sun, and T.H.Hyde1** 2009: Determination of material properties in the Chaboche unified viscoplasticity model

[6]**Ambroziak, Andrezej,**2005: Numerical Modelling of Elasto-Viscoplastic Chaboche Constıtutive Equations Using MSC. Marc

[7]**Schijve, Jaap,** 2001: Fatigue of Structures and Materials, Print ISBN 0-7923-7013-9, Kluwer Academic Publishers,2004

[8]**T. Seiferta, G. Maiera, A. Uihleinb, K. H. Langb, H. Riedel,**2008: Mechanism-based thermomechanical fatigue life prediction of cast iron.

[9]**Thomas Seifert,** 2006**:** Manual of the material routine ThoMat 2006

[10] **Marquard & Sorger**, 1997: AVL’s workshoop

[11]**Martin, T; Weber, R; Kaiser, R.W.**, 2003: Dünnwandige Zylinderblöcke aus Gusseisen, pp. 357-362.

[12**]Mario Metgezer, Fraunhofer IWM**, 2011: Computational methods for fatigue life estimation of cylinder heads made of vermicular cat iron

CURRICULUM VITAE

Name Surname	**:**	Şener KANTÜRER
Place and Date of Birth	**:**	Kırklareli, 24.05.1985
Address	**:**	İkbaliye Mah. Moralı İbrahim Paşa Sok. No:16/10 Kadıköy/ İSTANBUL
E-Mail	**:**	kanturers@gmail.com
B.Sc.	**:**	Istanbul Technical University